การดูดซับกรดโอเลอิกโดยใช้ตัวดูดซับที่ทำจากแกลบข้าว

นางสาวเบญจลักษณ์ นราไชย

วิทยานิพนธ์นี้เป็นส่วนหนึ่งของการศึกษาตามหลักสูตรปริญญาวิทยาศาสตรมหาบัณฑิต
สาขาวิชาเคมี
มหาวิทยาลัยเทคโนโลยีสุรนารี
ปีการศึกษา 2557

ADSORPTION OF OLEIC ACID USING ADSORBENTS

DERIVED FROM RICE HUSK

Benjaluck Narachai
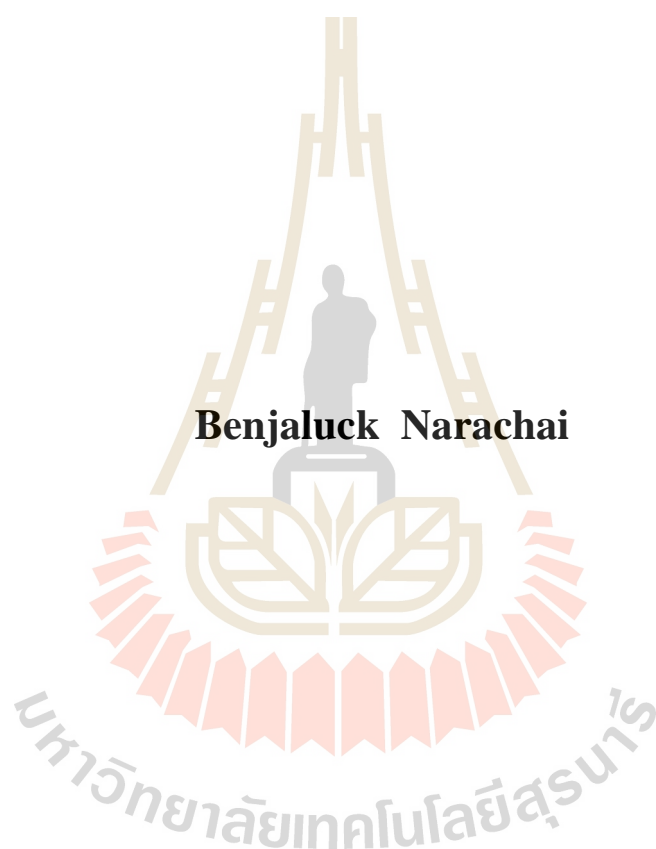
A Thesis Submitted in Partial Fulfillment of the Requirements for the

Degree of Master of Science in Chemistry

Suranaree University of Technology

Academic Year 2014

ADSORPTION OF OLEIC ACID USING ADSORBENTS

DERIVED FROM RICE HUSK

Suranaree University of Technology has approved this thesis submitted in partial fulfillment of the requirements for a Master's Degree.

Thesis Examining Committee

_____
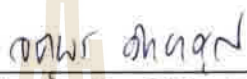
(Assoc. Prof. Dr. Jatuporn Wittayakun)

Chairperson

_____

(Asst. Prof. Dr. Sanchai Prayoonpokarach)

Member (Thesis Advisor)

_____

(Asst. Prof. Dr. Kunwadee Rangsriwatananon)

Member

_____

(Asst. Prof. Dr. Thanaporn Manyum)

Member

_____
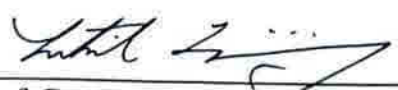
(Prof. Dr. Sukit Limpijumnong)

Vice Rector for Academic Affairs

and Innovation

_____

(Assoc. Prof. Dr. Prapun Manyum)

Dean of Institute of Science

เบญจลักษณ์ นราไชย : การดูดซับกรดโอเลอิกโดยใช้ตัวดูดซับที่ทำจากแกลบข้าว (ADSORPTION OF OLEIC ACID USING ADSORBENTS DERIVED FROM RICE HUSK) อาจารย์ที่ปรึกษา : ผู้ช่วยศาสตราจารย์ ดร.สัญชัย ประยูรโภคราช, 94 หน้า

กรดไขมันอิสระ (FFA) ในน้ำมันพืชที่กินได้และกินไม่ได้ที่ใช้สำหรับผลิตน้ำมันไบโอดีเซล สามารถทำปฏิกิริยากับตัวเร่งปฏิกิริยาเบส เป็นสาเหตุทำให้ผลได้น้ำมันไบโอดีเซลลดลง และตัวเร่งปฏิกิริยาเสื่อมสภาพ เพื่อช่วยลดปัญหาควรควบคุมความเข้มข้นของกรดไขมันอิสระให้ต่ำกว่า 1-2% โดยน้ำหนัก ดังนั้นการวิจัยนี้ จึงสนใจการแยกกรดไขมันอิสระในน้ำมันพืช โดยใช้ตัวดูดซับที่ทำจากซิลิกาจากแกลบข้าว และใช้กรดโอเลอิกเป็นตัวแทนของกรดไขมันอิสระ ตัวดูดซับคือ ซิลิกา, มอร์ดิไนต์ (MOR), MCM-41 ที่ไม่เผา [MCM-41 (A)] และ MCM-41 ที่เผา [MCM-41(C)] การทดลองการดูดซับทำแบบแบตช์ โดยใช้น้ำหนักตัวดูดซับคงที่ 0.25 กรัม ส่วนความเข้มข้นของกรด เวลา และอุณหภูมิที่ใช้ในการดูดซับแปรเปลี่ยนอยู่ในช่วง 0-3.00%, 0-3 ชั่วโมง และ 25-50 องศาเซลเซียส ตามลำดับ

ค่าความจุการดูดซับที่สมดุลที่อุณหภูมิ 25 องศาเซลเซียสของ MCM-41 (A) และ MCM-41 (C) มีค่า 277.8 มิลลิกรัมต่อกรัม และ 270.3 มิลลิกรัมต่อกรัม ตามลำดับ ค่าความจุการดูดซับของ MCM-41 (A) และ MCM-41 (C) มีค่ามากกว่ามอร์ดิไนต์ และซิลิกาประมาณ 4 เท่า การดูดซับกรดโอเลอิกบน MCM-41 (A) และ MCM-41 (C) เป็นไปตามแบบจำลองไอโซเทอร์มแบบแลงเมียร์ สำหรับ MCM-41 (A) มีค่าการเปลี่ยนแปลงเอนทัลปี (ΔH) และการเปลี่ยนแปลงเอนโทรปี (ΔS) เท่ากับ -3.59 กิโลจูลต่อโมล และ 21.5 จูลต่อโมล ตามลำดับ และสำหรับ MCM-41 (C) มีค่าเท่ากับ -7.22 กิโลจูลต่อโมล และ 9.07 จูลต่อโมล ตามลำดับ โดยค่าการเปลี่ยนแปลงพลังงานอิสระกิบส์ สำหรับกระบวนการดูดซับของตัวดูดซับทั้งสองนี้มีค่าเป็นลบที่ทุกอุณหภูมิการทดลอง

การใช้ MCM-41 (A) และ MCM-41 (C) ในการดูดซับกรดโอเลอิกในน้ำมันถั่วเหลือง แสดงให้เห็นว่าค่าความจุการดูดซับของ MCM-41 (A) มีค่าเท่ากับ 178.7 มิลลิกรัมต่อกรัม ในสารละลายกรดโอเลอิก 1% ในน้ำมันถั่วเหลือง ในขณะที่ไม่สังเกตพบการดูดซับดังกล่าวเมื่อใช้ MCM-41 (C)

สาขาวิชาเคมี	ลายมือชื่อนักศึกษา_____
ปีการศึกษา 2557	ลายมือชื่ออาจารย์ที่ปรึกษา_____

BENJALUCK NARACHAI : ADSORPTION OF OLEIC ACID

USING ADSORBENTS DERIVED FROM RICE HUSK. THESIS

ADVISOR : ASST. PROF. SANCHAI PRAYOONPOKARACH,

Ph.D. 94 PP.

FREE FATTY ACID, ADSORPTION, MCM-41, OLEIC ACID, RICE HUSK

SILICA

Free fatty acids (FFA) in edible and non-edible oils used for the production of

biodiesel can react with a basic catalyst and consequently, cause a lower biodiesel

yield and catalyst deactivation. To reduce the problems, the concentration of FFA in

the oil should be lower than 1-2 wt%. Therefore, in this research removal of FFA in

the oils using adsorbents derived from rice husk silica was studied. Oleic acid was

used as a representative of FFA. The adsorbents were rice husk silica, mordenite

(MOR), noncalcined MCM-41 [MCM-41 (A)] and calcined MCM-41 [MCM-41 (C)].

Adsorption experiments were performed in a batch mode using a fixed weight of the

adsorbent, 0.25 g. The concentration of the acid, the adsorption time and the

adsorption temperature were varied within the range of 0-3.0%, 0-3 h and 25-50 °C,

respectively.

The equilibrium adsorption capacities at 25 °C of MCM-41 (A) and MCM-41 (C)

were 277.8 mg/g and 270.3 mg/g, respectively. The adsorption capacities of MCM-41

(A) and MCM-41 (C) are about 4 times larger than those of mordenite and

III

rice husk silica. The adsorption of oleic acid onto MCM-41 (A) and MCM-41 (C) followed the Langmuir isotherm model. For MCM-41 (A), the enthalpy change (ΔH) and the entropy change (ΔS) were -3.59 kJ/mol and 21.5 J/mol, respectively, and those for the MCM-41 (C) were -7.22 kJ/mol and 9.07 J/mol, respectively. The values of the Gibbs free energy change (ΔG) for the adsorption process of both adsorbents were negative at all studied temperatures.

The application of MCM-41 (A) and MCM-41 (C) in the adsorption of oleic acid in soybean oil showed that the adsorption capacity of MCM-41 (A) was 178.7 mg/g in a solution of 1% oleic acid in soybean oil; whereas, no adsorption was observed using MCM-41 (C).
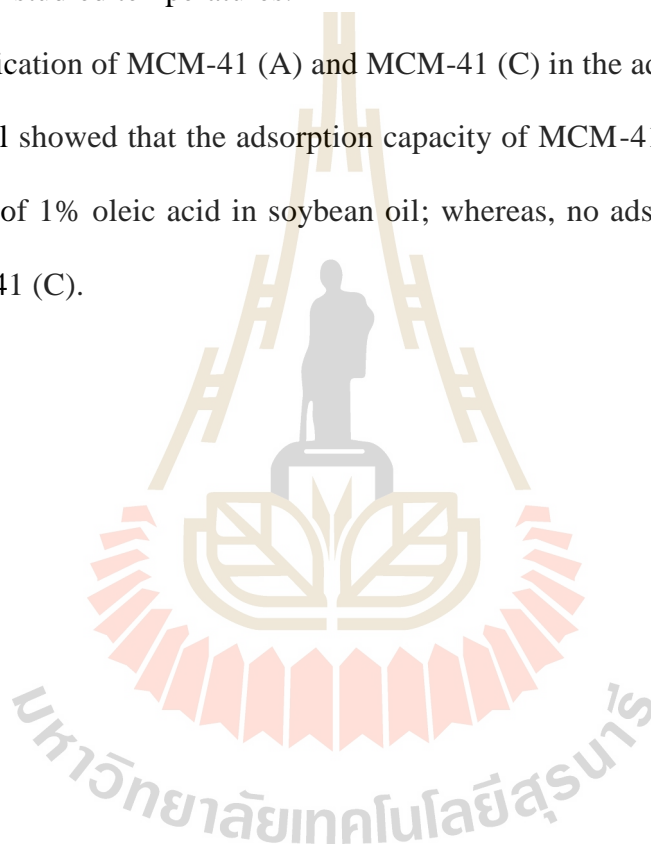
School of Chemistry   Student's Signature _____

Academic Year 2014   Advisor's Signature _____

ACKNOWLEDGEMENTS

CONTENTS

CONTENTS (Continued)

CONTENTS (Continued)

LIST OF TABLES

LIST OF TABLES (Continued)

LIST OF FIGURES

LIST OF FIGURES (Continued)

LIST OF FIGURES (Continued)

LIST OF FIGURES (Continued)

CHAPTER I

INTRODUCTION

1.1 Introduction

Vegetable oils from many plants such as soybean, palm and jatropha have been used as reactants for the production of biodiesel. The extracted crude oil from the plants is a mixture of many compounds, including free fatty acids (FFA) (Bhosle and Subramanian, 2005). In transesterification using a basic catalyst, FFA content in the oil should not exceed 1 wt%, because the FFA will react with the catalyst to form soap (Demirbaş, 2003; Zhang et al., 2010). The reaction will reduce the amount of the catalyst and the formation of soap will cause a difficulty in separation of biodiesel from the reaction mixture; consequently, these will lower the biodiesel yield. Therefore, it is important to remove or reduce the FFA in the oil. Besides causing the problem in biodiesel production, the presence of FFA in edible oils is also a problem in food, due to their effects on food spoilage and off flavor (rancidity) (Keurentjes, Doornbusch and Van't riet, 1991). Consequently, the removal of FFA will improve the oil quality to be used in the food industry. In this research, adsorption of FFA using adsorbents derived from rice husk silica (RHS) was investigated.

1.2 Adsorption

Adsorption is a phenomenon that results in the accumulation of molecules on a surface of a solid and a structure of the solid is not changed. The solid that accumulates other compounds on its surface is called adsorbent and the compound adsorbed on the adsorbent surface is called adsorbate. Adsorption involves a physical or chemical process. In physical adsorption, no chemical bonds are formed and the adsorption between the adsorbate and the adsorbent occurs from weak intermolecular forces. Chemical adsorption on the other hand, the adsorbate chemically bonds with the adsorbent surface. The amount adsorbed depends on the physical and chemical nature of the adsorbent. Porous solids are usually used in an adsorption process because high surface area or high pore volume increases the chance for the adsorbent and the adsorbate to come into contact and consequently, lead to high adsorption capacity.

The adsorption is based on three mechanisms which are steric, equilibrium and kinetic mechanisms. In the steric mechanism, the adsorbent has pore dimension that restricts to the molecules with certain size or shape. The equilibrium mechanism depends on the different ability of the molecules accumulate on the surface of the adsorbent. The kinetic mechanism is based on the rate of diffusion of molecules into the pore, which is controlled by the time of exposure on active sites (Do, 1998a).

1.2.1 Adsorption at the liquid-solid interface

Adsorption equilibrium will be achieved when the rate of adsorption is equal to the rate of desorption of the adsorbate from the surface of the adsorbent. The amount of the adsorbate bound to the adsorbent is usually measured at a constant temperature. A relationship of the binding of the adsorbate to the adsorbent at a constant temperature

is generally expressed as a curve called an adsorption isotherm. Langmuir and
Freundlich isotherm equations are commonly used to describe the adsorption behavior
(Demirbas, Sari and Isildak, 2006).

1.2.1.1 Langmuir isotherm

The Langmuir isotherm is used to describe equilibrium adsorption
based on three major assumptions (Do, 1998b), which are:

1. the surface of the adsorbent is homogenous; therefore, adsorption
energy is constant for all sites,

2. only one molecule or atom can be adsorbed on any one site and
adsorption cannot occur beyond a monolayer and

3. there is no interaction between any of the adsorbed molecules or
atoms.

The Langmuir adsorption equation can be represented as equation [1];

$$\frac{q}{q_m} = \frac{K_A X_e}{1 + K_A X_e} \tag{[1]}$$

where, q (mg/g) is the amount of the adsorbate adsorbed per gram of the adsorbent; q_m
(mg/g) is the amount of the adsorbate adsorbed to form a monolayer coverage; K_A
(L/mg) is the Langmuir adsorption equilibrium constant; X_e (mg/L) is the amount of the
adsorbate in a solution at equilibrium.

Adsorption data can be fitted to the Langmuir isotherm in its linear
form as equation [2];

$$\frac{X_e}{q} = \frac{X_e}{q_m} + \frac{1}{K_A q_m} \tag{[2]}$$

The suitability of the adsorbent to the adsorbate can be evaluated by using the Langmuir constant to calculate a value known as the constant separation factor, R_L as shown in equation [3];

$$R_L = \frac{1}{1 + K_A X_0} \qquad [3]$$

where, X_0 (mg/L) is the initial amount of adsorbate in a solution.

The value of R_L can be used to indicate the adsorption situations to be unfavorable ($R_L > 1.0$), linear ($R_L = 1.0$), irreversible ($R_L = 0$) and favorable ($0 < R_L < 1.0$) (Hall et al. 1966).

1.2.1.2 Freundlich isotherm

The Freundlich isotherm is another commonly used model. It has a general form as expressed by equation [4];

$$q = K_F X_e^{1/n} \qquad [4]$$

where q and X_e are the same as described in equation [1], K_F is the Freundlich constant, indicative of the relative adsorption capacity of the adsorbent and 1/n is an empirical constant.

By taking logarithm of equation [4], a linear form of Freundlich isotherm is shown in equation [5];

$$\ln q = \ln K_F + \frac{1}{n} \ln X_e \qquad [5]$$

When ln q is plotted against ln X_e and the data are treated by linear regression analysis, K_F and 1/n can be calculated from the intercept and a slope of the line, respectively. Freundlich model applies well to solid with heterogeneous surface properties.

1.2.2 Thermodynamic study

Thermodynamic parameters including Gibbs free energy change (ΔG), enthalpy change (ΔH) and entropy change (ΔS) are useful in providing the information about the adsorption process. Relationship among a distribution coefficient (K_D), ΔH and ΔS can be described by equation [6];

$$\ln K_D = \frac{\Delta S}{R} - \frac{\Delta H}{RT} \qquad [6]$$

where, R is the universal gas constant, (8.314 Jmol^{-1} K^{-1}); and T is the absolute temperature (Kelvin) and K_D can be calculated from equation [7];

$$K_D = \frac{q}{C_f} \qquad [7]$$

With q described by equation [8];

$$q = \frac{V(C_i - C_f)}{m} \qquad [8]$$

where C_i and C_f are the initial and equilibrium concentrations of the solute (mg/L) respectively, V is the volume of the solution (L) and m is the adsorbent mass (g).

The values of ΔH and ΔS can be calculated from the slope and the intercept of van't Hoff plot of $\ln K_D$ against 1/T.

The Gibbs free energy change, ΔG, provides information about the process spontaneity, which can be related to ΔH and ΔS as shown in equation [9];

$$\Delta G = \Delta H - T\Delta S \qquad [9]$$

The Gibbs free energy change can also be determined using the relation as follows: $\Delta G = -RT \ln K_D$ \qquad [10]

The effects of the enthalpy change, entropy change and temperature on spontaneity of a reaction are summarized in Table 1.1.

Table 1.1 The contribution of the enthalpy, entropy, Gibbs free energy change and temperature on spontaneity of a reaction (Zumdahl, S. S. and Zumdahl, S. A., 2007).

ΔH	ΔS	ΔG	Spontaneity of a process
$-$	$+$	$-$	Spontaneous at all temperature
$+$	$-$	$+$	Non-spontaneous
$+$	$+$	$-$	Spontaneous only at high temperature
$-$	$-$	$-$	Spontaneous only at low temperature

1.3 Adsorbents

The adsorbent is an important variable in the adsorption process. The success of the process relies on the adsorbent performance in both equilibrium and kinetics. Porous solids with small particle sizes and a reasonable porosity could be the good adsorbents, as they could provide high adsorption capacity and aid the fast kinetics. The pore size of porous solids was classified by the International Union of Pure and Applied Chemistry (IUPAC) based on the average pore size as shown in Table 1.2.

Table 1.2 IUPAC pore classification.

Type of pores	Mean pore diameter (Å)
Micropore	< 20
Mesopore	$20 - 500$
Macropore	> 500

1.3.1 Rice husk silica (RHS)

Silicon dioxide (SiO_2) or silica has a structure of silicon atom tetrahedrally bonded to four oxygen atoms and each oxygen atom is shared with other silicon atom. Silica has relatively high thermal and chemical stability. A number of different crystalline forms such as quartz and cristobalite are present in addition to an amorphous form.

Silica can be produced from rice husk and its application in adsorption has been reported by many researchers. Acid leaching by hydrochloric acid and sulfuric acid has been used to recover silica from rice husk (Yalçin and Sevinç, 2001). In this method, rice husk was treated with the acid, washed with water, dried and calcined at 600 °C. A method based on alkaline extraction was also studied (Kalapathy, Proctor and Shultz, 2002). Rice husk was boiled in a sodium hydroxide solution to dissolve the silica out. The solution was separated from the husk and hydrochloric acid was added in to the solution to precipitate the silica.

The surface of silica has silanol groups (Si-OH) which are responsible for its reactivity. The surface can be organically modified to alter the polarity for a certain application.

1.3.2 Mordenite (MOR)

Zeolite is a microporous crystalline aluminosilicate compound consisted of tetrahedral SiO_4 and AlO_4 unit in a framework. At locations where Si^{4+} is substituted by Al^{3+}, the framework carries a negative charge. The negative charge sites are balanced by cations, usually alkali and alkaline earth metals. The arrangement of three-dimensional framework structure leads to the formation of uniform pores. Typically, the pore diameters are between 3 and 10 Å. The cation exchange capability and the open

cavity of the zeolites have contributed to many applications such as a molecular sieve and an adsorbent for saturated and unsaturated hydrocarbons (Pantu, Boekfa and Limtrakul, 2007).

MOR is one of the high silica zeolites. It has two channel sizes, 6.7 Å $\times$ 7.0 Å and 2.6 Å $\times$ 5.7 Å, which are not interconnected. The former channel is formed by 12 tetrahedral units (SiO_4) and the latter is generated from 8 tetrahedra (SiO_4 and AlO_4); therefore, the channels are called 12- and 8-membered ring channels, respectively.

MOR has been used as a catalyst in many petrochemical processes and an adsorbent for adsorption. Pantu et al. (2007) used MOR to adsorb saturated and unsaturated hydrocarbons. The adsorption was due to the acid sites of the zeolite, the van der Waals interaction and the different pore sizes of the zeolite. Sato, Kudo and Tsuda (2011) used MOR to remove radioactive contaminants such as cesium, strontium and barium ions in drinking water. The mechanism responsible for the removal is ion exchange between zeolite counter cations and these contaminants.

Kulawong, Prayoonpokarach, Neramittagapong and Wittayakun (2011) synthesized MOR in sodium form (NaMOR) by mixing a solution of RHS in sodium hydroxide and a solution of sodium aluminate. The mixture in a polypropylene bottle was stirred at room temperature for one day or until the RHS was dissolved completely. The obtained mixture with an original molar composition of 2.5 Na_2O: Al_2O_3: 22SiO_2: 518H_2O was then transferred to a Teflon-lined stainless steel autoclave for crystallization at 170 °C for four days. The solid product was separated, washed thoroughly with deionized water, dried at 80 °C overnight and calcined in a muffle

furnace at 500 °C for 3 h. The obtained zeolite was reported to have a surface area of 414 m^2/g.

1.3.3 MCM-41

MCM-41 is a mesoporous material consisted of silica framework with hexagonal array of cylindrical pores whose dimensions are in the range of 15 Å to greater than 100 Å and the surface area is above 700 m^2/g (Beck et al., 1992). MCM-41 possesses a hydrophobic property (Serrano, Calleja, Botas and Gutierrez, 2004) which is particularly useful for the separation of organic compounds or nonpolar substances. Its structural and chemical characteristics make the material properties beneficial for adsorption (Grün, Unger, Matsumoto and Tsutsumi, 1999) and separation technologies (Grün, Kurganov, Schacht, Schüth and Unger, 1996).

MCM-41 is used in many applications such as a support for catalysts (Grün et al., 1999) and an adsorbent for various gases and volatile organic compounds (VOCs) (Hu, Qiao, Zhao and Lu, 2001). In addition, the surfactant contained MCM-41 has been used for removal of nonionic organic compounds such as benzene, toluene and phenol from contaminated wastewater (Ghiaci, Abbaspur, Kai and Seyedeyn-Azad, 2004).

MCM-41 can be produced from RHS and the synthesized condition has been reported (Rintramee, Föttinger, Rupprechter and Wittayakun, 2012). A silicate solution obtained from RHS dissolved in a sodium hydroxide solution was mixed at room temperature with a solution of cetyltrimethyl ammonium bromide (CTAB) used as a template. The pH of the mixture was adjusted to 11 using 2.5 M sulfuric acid (H_2SO_4) and it was stirred for 4 h in a polypropylene bottle. The mixture was transferred to a Teflon-lined stainless steel autoclave and heated at 100 °C for three days. The solid

product was separated, washed thoroughly with deionized water, dried at 100 °C for 24 h and calcined in a muffle furnace at 540 °C for 6 h.

The formation of MCM-41 structure can be explained by two mechanistic pathways. In the first pathway, the surfactant molecules form micelles and then the siliceous framework polycondenses around the micelles. This process is called liquid crystal initiated pathway. In the second pathway, the anionic siliceous associates with the surfactant and then polycondenses to form the MCM-41 structure. This mechanism is called anion-initiated pathway. Calcination of the final product removes the surfactant template to create a mesoporous material with a highly ordered array of pores of well-defined size.

In this research adsorbents derived from rice husk, which are RHS, MOR and MCM-41, were synthesized, characterized, and studied for their capability to adsorb oleic acid. Parameters such as acid concentration, time and temperature that could influence the adsorption efficiency were investigated.

1.4 References

Beck, J. S.,Vartuli, J. C., Roth, W. J., Leonowicz, M. E., Kresge, C. T., Schmitt, K. D., Chu, C. T-W., Olson, D. H., Sheppard, E. W., McCullen, S. B., Higgins, J. B., and Schlenker, J. L. (1992). A new family of mesoporous molecular sieves prepared with liquid crystal templates. **Journal of the American Chemical Society**. 114: 10834-10843.

Bhosle, B. M. and Subramanian, R. (2005). New approaches in deacidification of edible oils-A review. **Journal of Food Engineering**. 69: 481-494.

Demirbaş, A. (2003). Biodiesel fuels from vegetable oils via catalytic and non-

catalytic supercritical alcohol transesterifications and other methods: A survey. **Energy Conversion and Management**. 44: 2093-2109.

Demirbas, A., Sari, A., and Isildak, O. (2006). Adsorption thermodynamics of stearic acid onto bentonite. **Journal of Hazardous Materials**. 135: 226-231.

Do, D. D. (1998a). **Adsorption analysis: Equilibria and kinetic**. (pp. 1-2). Singapore: World Scientific Publishing Co. Pte. Ltd.

Do, D. D. (1998b). **Adsorption analysis: Equilibria and kinetic**. (p. 13). Singapore: World Scientific Publishing Co. Pte. Ltd.

Ghiaci, M., Abbaspur, A., Kai, R., and Seyedeyn-Azad, F. (2004). Equilibrium isotherm studies for the sorption of benzene, toluene, and phenol onto organo-zeolites and as-synthesized MCM-41. **Separation and Purification Technology**. 40: 217-229.

Grün, M., Kurganov, A. A., Schacht, S., Schiith, F., and Unger, K. K. (1996). Comparison of an ordered mesoporous aluminosilicate, silica, alumina, titania and zirconia in normal-phase high-performance liquid chromatography. **Journal of Chromatography A**. 740: 1-9.

Grün, M., Unger, K. K., Matsumoto, A., and Tsutsumi, K. (1999). Novel pathways for the preparation of mesoporous MCM-41 materials: Control of porosity and morphology. **Microporous and Mesoporous Materials**. 27: 207-216.

Hu, X., Qiao, S., Zhao, X. S., and Lu, G. Q. (2001). Adsorption study of benzene in Ink-Bottle-Like MCM-41. **Industrial & Engineering Chemistry Research**. 40: 862-867.

Kalapathy, U., Proctor, A., and Shultz, J. (2002). An improved method for production of silica from rice hull ash. **Bioresource Technology**. 85: 285-289.

Keurentjes, J. T. F., Doornbusch, G. I., and Van't riet, K. (1991). The removal of fatty acids from edible oil. Removal of the dispersed phase of water-in-oil dispersion by a hydrophilic membrane. **Separation Science and Technology**. 26(3): 409-423.

Kulawong, S., Prayoonpokarach, S., Neramittagapong, A., and Wittayakun, J. (2011). Mordenite modification and utilization as supports for iron catalyst in phenol hydroxylation. **Journal of Industrial and Engineering Chemistry**. 17: 346-351.

Pantu, P., Boekfa, B., and Limtrakul, J. (2007). The adsorption of saturated and unsaturated hydrocarbons on nanostructured zeolites (H-MOR and H-FAU): An ONIOM study. **Journal of Molecular Catalysis A: Chemical**. 277: 171-179.

Rintramee, K., Föttinger, K., Rupprechter, G., and Wittayakun, J. (2012). Ethanol adsorption and oxidation on bimetallic catalysts containing platinum and base metal oxide supported on MCM-41. **Applied Catalysis B: Environmental**. 115-116: 225-235.

Sato, I., Kudo, H., and Tsuda, S. (2011). Removal efficiency of water purifier and adsorbent for iodine, cesium, strontium, barium and zirconium in drinking water. **The Journal of Toxicological Sciences**. 36 (6): 829-834.

Serrano, D. P., Calleja, G., Botas, J. A., and Gutierrez, F. J. (2004). Adsorption and hydrophobic properties of mesostructured MCM-41 and SBA-15 materials for volatile organic compound removal. **Industrial and Engineering Chemistry Research**. 43: 7010-7018.

Yalçin, N. and Sevinç, V. (2001). Studies on silica obtained from rice husk. **Ceramics International**. 27: 219-224.

Zhang, S., Zu, Y-G., Fu, Y-J., Luo, M., Zhang, D-Y., and Efferth, T. (2010). Rapid microwave-assisted transesterification of yellow horn oil to biodiesel using a

heteropolyacid solid catalyst. **Bioresource Technology**. 101: 931-936.

Zumdahl, S. S. and Zumdahl, S. A. (2007). **Chemistry**. (7th ed., pp. 796-800). Boston: Houghton Mifflin Company.
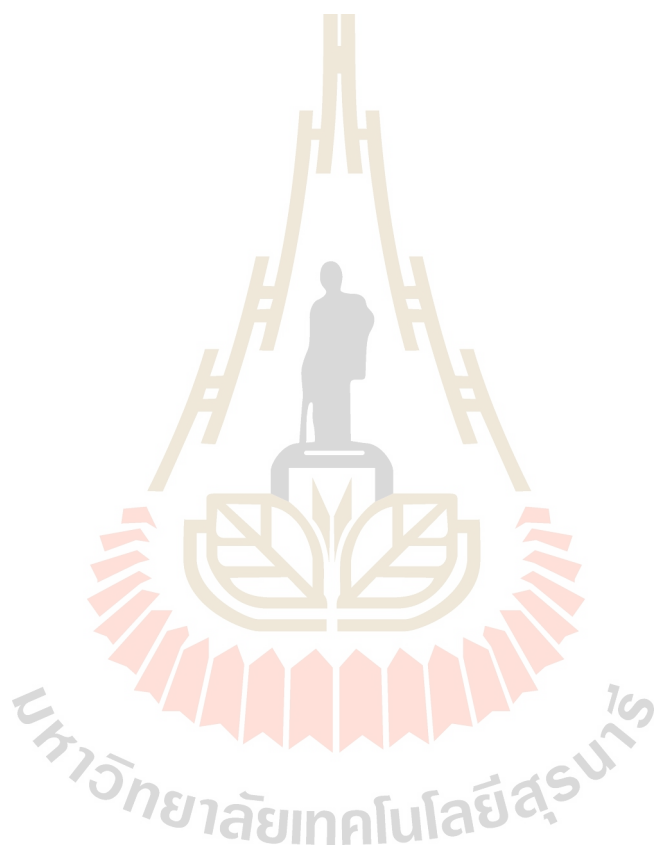
CHAPTER II

LITERATURE REVIEWS

2.1 Introduction

Free fatty acids (FFA) in vegetable oils are classified according to their degree of saturation. The types of FFA are saturated acids whose molecules contain only single carbon-to-carbon bond, such as palmitic acid and stearic acid and unsaturated acids whose molecules have one or more carbon-to-carbon double bonds, such as linoleic acid, oleic acid and linolenic acid. FFA in the vegetable oils can be derived from triglycerides which compose of different fatty acids moiety dependent on their origins. Fatty acid compositions of some vegetable oils are summarized in Table 2.1.

Table 2.1 Fatty acid compositions (%wt) of some vegetable oils (Demirbaş, 2003).

Oil	Palmitic C16:0[a]	Palmitoleic C16:1	Stearic C18:0	Oleic C18:1	Linoleic C18:2	Linolenic C18:3	Others
Rape seed	3.5	0	0.9	64.1	22.3	8.2	0
Sunflower seed	6.4	0.1	2.9	17.7	72.9	0	0
Sesame seed	15.2	0	6.8	44.6	30.2	0.2	0
Palm	42.6	0.3	4.4	40.5	10.1	0.2	1.1
Soybean	13.9	0.3	2.1	23.2	56.2	4.3	0
Olive kernel	5.0	0.3	1.6	74.7	17.6	0	0.8

[a] A symbol Cn:x represents the molecule of a fatty acid with the number of n carbons and x double bonds.

From Table 2.1 C18 fatty acids are among the most abundant components in the vegetable oils; therefore, in this research, oleic acid was selected as a representative of the FFA for the adsorption study.

In recent years, there are many reports in removal of FFA from vegetable oils. Ramadhas, Jayaraj and Muraleedharan (2005) used esterification process with sulfuric acid as a catalyst to reduce the FFA content of the crude rubber seed oil. The crude rubber seed oil and methanol were mixed with 0.5%v/v of sulfuric acid/ oil at 50 °C for 20-30 min under atmospheric pressure. The amount of FFA was reduced from ~17 %wt to < 2 %wt.

Suppalakpanya, Ratanawilai and Tongurai (2010) performed esterification under a microwave heating technique by mixing crude palm oil and ethanol with 1.0 %wt of sulfuric acid/ oil. The mixture was heated at 70 W for 60 min. The FFA content was reduced from ~3-7 %wt to 1.7 %wt. SathyaSelvabala, Varathachary, Selvaraj, Ponnusamy and Subramanian (2010) studied the removal of FFA by using phosphoric acid modified mordenite (PMOR) as a catalyst in esterification of *Azadirachta indica* (Neem) seed oil. Neem seed oil and methanol were mixed with 1 %wt solid catalyst at 60 °C for 3 h. The acid value reduced from 24.4 to 1.8 mg KOH/g oil or 0.90 %wt (%FFA as oleic acid = (mg KOH/g oil)/1.99).

Sathya Selva Bala et al. (2012) used strong acidic ion exchange resins, Amberlite IR 120 and Amberjet 1200 H, as the catalyst in esterification to reduce FFA in *Pongamia Pinnata* (Karanja) oil. The acid value reduced from 12.5 to 1.6 and 1.72 mg KOH/g oil (FFA content of 0.8 and 0.86 w/w) for Amberlite IR 120 H and Amberjet 1200 H catalyzed esterification reaction, respectively. The reaction was conducted with

the catalyst concentration of 1 %wt, the temperature of 60 °C, the methanol to oil ratio of 6:1 and the reaction time of 150 min.

Martins, Ito, Batistella and Maciel (2006) used distillation process for reduction of FFA in vegetable oils. The removal percentage of FFA was 96.16% by using the feed flow rate at 10.4 g of oil/min and the evaporator temperature of 160 °C. The methods of esterification and distillation of FFA are not economical in terms of energy consumption.

Adsorption is another method for FFA removal that has advantages such as simple operating process and low operating cost. Many adsorbents, for example, rice husk ash (RHA) (Saleh and Adam, 1994), silica gel (Atia, El-Nahas, Marie and Mahdy, 2006), RHA and rice husk silica (RHS) (Kim, Yoon, Choi and Gil, 2008), acid treated RHA (Yoon, Kim and Gil, 2011), and mixed bed ion-exchange resins (Jamal and Boulanger, 2010) were used for adsorption of FFA. In this work, adsorbents derived from rice husk silica were used.

Rice husk is an agricultural waste largely generated in rice-producing countries. It contains ~ 25 %wt silica (Yalçin and Sevinç, 2001). Silica extracted from rice husk can be used as a silica source for the production of a number of silica based materials (Khemthong et al., 2007). RHA obtained from pyrolyzed rice husk has been investigated as an adsorbent for FFA (Kim et al., 2008). Silicate films produced from RHA were evaluated for adsorption of FFA in frying oil (Kalapathy and Proctor, 2000). Adsorption of FFA on the silica surface was explained to occur via hydrogen bonding between carboxyl groups of FFA and silanol groups of silica (Atia et al., 2006; Proctor, Adhikari and Blyholder, 1995).

Saleh and Adam (1994) used RHA heated at 480 °C for adsorption of lauric, myristic and stearic acids in isooctane and the adsorption capacities were 35.7 mg/g, 43.5 mg/g and 36.0 mg/g, respectively. The acid adsorption conformed to Langmuir isotherm. Atia and coworkers (2006) studied the adsorption of oleic acid in hexane using silica gel derived from RHA as an adsorbent and explained that the adsorption of oleic acid onto a silica surface occurs via hydrogen bonding between the carboxyl group of the acid and silanol group of the silica surface. The maximum adsorption capacity was 19.7 mg/g at 28 °C. The adsorption data agreed well with Langmuir isotherm. Kim and coworkers (2008) studied the adsorption of FFA in degummed soybean oil using adsorbents obtained from RHA calcined in the temperature range of 300-900 °C and silica gel synthesized using calcined RHA at 500 °C as a silica source. High pyrolysis temperature resulted in the decrease of surface area and pore volume of the RHAs except for RHA pyrolized at 500 °C that had the highest pore volume and highest adsorption capacity for FFA. The silica gel and RHA pyrolyzed at 500 °C have similar adsorption capacity. Similar studies were done by Yoon and coworkers (2011). In their studies, RHA was treated with 20 %v/v sulfuric acid and calcined at various temperatures. They found that RHA heated at 500 °C was the most efficient adsorbent among the pyrolyzed RHAs and exhibited no difference in ability in FFA adsorption compared with the acid treated RHA pyrolyzed at 500 °C.

Farook and Ravendran (2000) used RHA that was treated with 1.0 M and 14.0 M nitric acid as the adsorbents for saturated FFAs. RHA treated with 14.0 M nitric acid has higher adsorption capacities than that treated with 1.0 M nitric acid. This was attributed to the increase in specific pore volume. Langmuir isotherm was used to explain the behavior of the adsorption of the acids.

Adam and Chua (2004) studied adsorption of palmitic acid on silica-incorporated aluminium (RHA-Al) and RHA-Al calcined at 500 °C, RHA-Al (C). The maximum adsorption capacities of the RHA-Al were 15.48 mg/g at 30 °C, 15.92 mg/g at 40 °C and 16.64 mg/g at 50 °C. The maximum adsorption capacities of the RHA-Al (C) were 15.82 mg/g at 30 °C, 20.16 mg/g at 40 °C and 21.51 mg/g at 50 °C. The acid adsorption followed Langmuir isotherm. The Al incorporated into the silica matrix acted as Lewis acid responsible for the adsorption by interacting with the C=O of the acid.

From the literatures, it is clear that silica based materials derived from rice husk have been shown to be the potential adsorbents for the removal of FFA. It can also be inferred that the silica based materials with higher surface area than the silica could have higher adsorption capacity for the FFA. Therefore, in this research mordenite and MCM-41 derived from RHS were investigated as the adsorbents for the adsorption of oleic acid.

2.2 References

Adam, F. and Chua, J.-H. (2004). The adsorption of palmytic acid on rice husk ash chemically modified with Al(III) ion using the sol-gel technique. **Journal of Colloid and Interface Science**. 280: 55-61.

Atia, A. A., El-Nahas, A. M., Marie, A. M., and Mahdy, L. D. Al. (2006). Adsorption of oleic acid on silica gel derived from rice ash hulls: Experimental and theoretical studies. **Adsorption Science and Technology**. 24(9): 797-814.

Demirbaş, A. (2003). Biodiesel fuels from vegetable oils via catalytic and non-catalytic supercritical alcohol transesterifications and other methods: A survey. **Energy**

Conversion and Management. 44: 2093-2109.

Farook, A. and Ravendran, S. (2000). Saturated fatty acid adsorption by acidified rice hull ash. **Journal of the American Oil Chemists' Society**. 77: 437-440.

Jamal, Y. and Boulanger, B. O. (2010). Separation of oleic acid from soybean oil using mixed-bed resins. **Journal of Chemical and Engineering Data**. 55: 2405-2409.

Kalapathy, U. and Proctor, A. (2000). A new method for free fatty acid reduction in frying oil using silicate films produced from rice hull ash. **Journal of the American Oil Chemists' Society**. 77(6): 593-598.

Khemthong, P., Prayoonpokarach, S., and Wittayakun, J. (2007). Synthesis and characterization of zeolite LSX from rice husk silica. **Suranaree Journal of Science and Technology**. 14(4): 367-379.

Kim, M., Yoon, S. H., Choi, E., and Gil., B. (2008). Comparison of the adsorbent performance between rice hull ash and rice hull silica gel according to their structural differences. **Food Science and Technology**. 41: 701-706.

Martins, P. F., Ito, V. M., Batistella, C. B., and Maciel, M. R. W. (2006). Free fatty acid separation from vegetable oil deodorizer distillate using molecular distillation process. **Separation and Purification Technology**. 48: 78-84.

Proctor. A., Adhikari, C., and Blyholder, G.D. (1995). Mode of oleic acid adsorption on rice hull ash cristobalite. **Journal of the American Oil Chemists' Society**.72: 331-335.

Ramadhas, A. S., Jayaraj, S., and Muraleedharan, C. (2005). Biodiesel production from high FFA rubber seed oil. **Fuel**. 84: 335-340.

Saleh M. I. and Adam, F. (1994). Adsorption isotherms of fatty acids on rice hull ash in

a model system. **Journal of the American Oil Chemists' Society**. 71(12): 1363-1366.

Sathya Selva Bala, V., Thiruvengadaravi, K.V., Senthil Kumar, P., Premkumar, M.P., Vinoth kumar, V., Subash sankar, S., Hari Kumar, M., and Sivanesan, S. (2012) Removal of free fatty acids in Pongamia Pinnata (Karanja) oil using divinylbenzene-styrene copolymer resins for biodiesel production. **Biomass and Bioenergy**. 37: 335-341.

SathyaSelvabala, V., Varathachary, T. K., Selvaraj, D. K., Ponnusamy, V., and Subramanian, S. (2010). Removal of free fatty acid in *Azadirachta indica* (Neem) seed oil using phosphoric acid modified mordenite for biodiesel production. **Bioresource Technology**. 101: 5897-5902.

Suppalakpanya, K., Ratanawilai, S. B., and Tongurai, C. (2010). Production of ethyl ester from esterified crude palm oil by microwave with dry washing by bleaching earth. **Applied Energy**. 87: 2356-2359.

Yalçin, N. and Sevinç, V. (2001). Studies on silica obtained from rice husk. **Ceramics International**. 27: 219-224.

Yoon, S. H., Kim, M., and Gil, B. (2011). Deacidification effects of rice hull-based adsorbents as affected by thermal and acid treatment. **LWT - Food Science and Technology**. 44: 1572-1576.

CHAPTER III

EXPERIMENTAL

3.1 Chemicals

Chemicals used in this research were purchased from various suppliers as shown in Table 3.1. All chemicals were used as received with no further purification.

3.2 Preparation of adsorbents

3.2.1 Rice husk silica

Rice husk silica (RHS) was prepared from the method reported in the literature (Khemthong et al., 2007; Kulawong et al., 2011). Rice husk was washed thoroughly with water to remove adhering soil and dust. After that the rice husk was dried at 100 °C overnight. Dried rice husk, 85 g, was refluxed with 700 mL of 3.0 M HCl in a round-bottomed glass flask at 85 °C for 3 h. After the acid reflux, the color of the rice husk changed from brown to black. The treated rice husk was separated from the solution and washed with water several times until the pH of the filtrate was ~7. The treated rice husk was dried at 100 °C overnight and then calcined in a muffle furnace at 550 °C for 6 h to remove hydrocarbons and volatile compounds. A white powder product was obtained and called rice husk silica. The obtained RHS was ground in a grinder, sieved to the particle sizes of 63-75 μm and kept at room temperature in a desiccator.

Table 3.1 Chemicals used in this work.

Chemicals	% content	Supplier
acetonitrile	99.9	Carlo ERBA
ethyl alcohol	99.9	Carlo ERBA
glacial acetic acid	99.9	J.T.Baker
hexadecyltrimethyl ammonium bromide (CTAB)	99.0	Acros
hydrochloric acid	36.5	Carlo ERBA
isooctane	99.5	Carlo ERBA
isopropyl alcohol	99.5	Carlo ERBA
oleic acid	90.0	Sigma-Aldrich
phenolphthalein	-	QRec
potassium hydrogen phthalate	99.95-100.0	Sigma-Aldrich
potassium hydroxide	85.0	QRec
sodium aluminate	40.0-45.0 Na_2O, 50.0-60.0 Al_2O_3	QRec
sodium hydroxide	97.0	Carlo ERBA
sulfuric acid	96.0-98.0	QRec
toluene	99.5	Carlo ERBA

3.2.2 Mordenite

Mordenite (MOR) in sodium form (NaMOR) was synthesized according to the literature (Kulawong et al., 2011). Sodium aluminate, 4.76 g, and 14 mL of 11.3 M NaOH were mixed with stirring provided for 30 min in a polypropylene bottle and 215 mL of deionized water was later added. The mixture was later stirred continuously for another 30 min. After that, 32.7 g of RHS was added and the mixture was stirred at room temperature for 1 day or until the solid was completely dissolved. The clear solution

was transferred to a Teflon-lined stainless steel autoclave with 250 mL capacity for crystallization at 170 °C for 4 days. A solid product obtained was separated by filtration and washed thoroughly with deionized water until the pH of the filtrate was ~7. The solid was dried at 80 °C overnight. The white powder product was ground in a grinder, sieved to the particle sizes of 63-75 μm and kept at room temperature in a desiccator.

3.2.3 MCM-41

Mobil Composition of Matter No.41 (MCM-41) was synthesized using a method from the literature (Rintramee et al., 2012). A 3.0 g of RHS was mixed with 30 mL of 5 M NaOH under stirring in a polypropylene bottle until the RHS was dissolved completely and the solution was added to 90 mL of 0.14 M CTAB solution with stirring provided at room temperature. The solution pH was adjusted to 11-12 by slowly adding 2.5 M H_2SO_4. The solution was transferred to a Teflon-lined stainless steel autoclave with 250 mL capacity and heated at 100 °C for 3 days. The solid product obtained was separated by centrifugation, washed thoroughly with deionized water until the pH of the filtrate was ~7. The obtained solid was dried at 100 °C.

To remove CTAB, the solid product was calcined in a muffle furnace at 540 °C for 6 h and the obtained solid is denoted as MCM-41 (C). For MCM-41 without template removal, it is called MCM-41 (A). Both forms of MCM-41 were ground in a grinder, sieved to the particle sizes of 63-75 μm and kept at room temperature in a desiccator.

3.3 Characterization of the adsorbents

X-ray diffraction (XRD) patterns of the synthesized adsorbents were obtained from a Bruker-AXS D5005 diffractometer to gain the structural information of the adsorbents. A sample of about 0.20 g was irradiated with the X-ray from Cu K_α with the source operated at 40 kV and 40 mA. For MCM-41 samples a scan range was 1.5 to 10.0° (2θ) and for silica and MOR the scan range was 5.0 to 50.0° (2θ). A scan speed of 0.5° per min was used for all adsorbents.

The surface area, pore volumes and pore sizes were determined by nitrogen adsorption-desorption analysis at -196 °C using a Micromeritics ASAP 2010. The sample weights of 0.18-0.20 g were used. MCM-41 (A) was degassed at 250 °C for 2 h (Jabariyan and Zanjanchi, 2012) and MCM-41 (C) was degassed at 300 °C for 4 h (Rintramee et al., 2012). The degassed temperature and time were 300 °C and 12 h for MOR (Kulawong et al., 2011) and silica (Artkla et al., 2008).

The specific surface area (S_{BET}) was calculated by Brunauer-Emmett-Teller (BET) method in the relative adsorption pressure (P/P_0) range from 0.001 to 0.990 for all samples. The total pore volume (V_t) was obtained from the nitrogen amount adsorbed in correspondence of P/P_0 equal to 0.99 and the pore size distributions calculated by Barrett-Joyner-Halenda (BJH) method.

The adsorbents were characterized by FTIR to identify functional groups in the structure. FTIR spectra were recorded before and after oleic acid adsorption on a Bruker IR spectrometer, TENSOR 27. To prepare a sample for an IR measurement, a homogeneous mixture between the adsorbent and potassium bromide (KBr) powder ratio 1:6 was ground in a mortar. Small amount of the ground mixture was transferred into a stainless steel disks set and a hydraraulic pressure was applied onto the sample

for 1 min to form a thin and transparent pellet. The pellet was put onto the sample holder of the FTIR spectrometer for the transmittance measurements in the range 400-4000 cm^{-1} with the resolution of 4 cm^{-1}.

^{29}Si MAS NMR spectra of MCM-41 samples were obtained with a Bruker nuclear magnetic resonance spectrometer (Ascend^{TM} 500, 500 MHz) equipped with a 4 mm probe (MAS BB/1H/F19/F19) and zirconia rotors. The measurement were performed at an operation field of 11.7 Tesla, a frequency at 99.39 MHz, a pulse duration of 4 μs, a recycle delay of 5.0 s and 12000 scans. The spectra were referenced to kaolin (δ = -93.1 ppm).

3.4 Preparation of solutions

3.4.1 Potassium hydroxide solutions

Potassium hydroxide (KOH) was used for the titration of oleic acid. A stock solution of 0.1 M KOH was prepared by dissolving 1.65 g of KOH in 250 mL of carbon dioxide-freed deionized water. A solution of 0.01 M KOH was prepared by the dilution of the 0.1 M KOH solution. The solution was standardized with potassium hydrogen phthalate using 1% phenolphthalein solution as the indicator.

3.4.2 Phenolphthalein indicator

Phenolphthalein was used as an indicator for the titration of KOH and oleic acid. To prepare 1% w/v phenolphthalein, 1.0 g of phenolphthalein was dissolved in 50 mL of ethanol. The solution was transferred into a 100 mL volumetric flask and the volume of the solution was adjusted with carbon dioxide-free deionized water.

3.4.3 Toluene and isopropanol solution

A mixture of toluene and isopropanol with 1:1 volume ratio was used as a solvent for the titration of oleic acid in isooctane and in vegetable oil. Before using in the titration, the solution was neutralized with a standardized 0.1 M KOH using phenolphthalein as the indicator.

3.5 Adsorption studies

Solutions of oleic acid in isooctane with the concentrations in the range of 0.10-3.00 %w/v were used in the adsorption isotherm study. To 25 mL of the oleic acid solution, an adsorbent (predried at 110 °C and cooled) weight of 0.25 g was added. The mixture contained in a 125 mL erlenmeyer flask was placed into a flask clamp mounted on a platform inside a stainless steel water bath. The water bath dimension was 35.5 cm (L) × 45.0 cm (W) × 12.0 cm (H). The water bath was connected to a temperature controlled water bath (Heto Lab Equipment, AT110). Stirring was provided to the adsorption mixture using a multiposition stirrer (DiLigent) for 60 min. After stirring was stopped for 30 s, the adsorbent was separated from the oleic acid solution by gravitation. The clear solution was used for determination of oleic acid by titration with 0.01 M KOH.

Effect of adsorption time on the adsorption capacity was investigated in the time range of 10-180 min. The temperature for the adsorption study was fixed at 25 °C. Solutions of oleic acid in isooctane with the concentration of 0.50 %w/v, the adsorbent weight of 0.50 g were used in the adsorption study.

Influence of temperature on the adsorption was investigated in the temperature range of 25-50 °C. The concentration of oleic acid in isooctane was 0.50 %w/v and the weight of the adsorbent was 0.25 g.

3.6 Determination of oleic acid

3.6.1 Titration

The oleic acid concentration in a solution was determined using the American Oil Chemists' Society method for the determination of free fatty acid (AOCS Ca 5a 40). The volume of oleic acid solution and the solvent mixture of toluene and isopropyl alcohol used in the titration are shown in Table 3.2.

Table 3.2 Volumes of oleic acid solutions used in the titration.

Concentration of oleic acid (%w/v)	Volume of oleic acid (mL)	Volume of toluene/isopropyl solution (mL)
0.10	2.00	25.0
0.50	2.00	25.0
1.00	0.50	25.0
2.00	0.50	25.0
2.50	0.50	50.0
3.00	0.50	50.0

3.6.2 High performance liquid chromatography (HPLC)

High performance liquid chromatography (Agilent 1260 Infinity) equipped with standard autosampler (G1315D) and a diode array detector was used for the determination of oleic acid in the adsorption studies that used MOR as the adsorbent. The method used was modified from the literature (Sanches-Silva et al., 2004).

A reversed phase Hypersil ODS C-18 column (250 mm × 4.0 mm i.d., particle size 5 μm) was used for separation of oleic acid and a mobile phase was acetonitrile mixed with 0.4% acetic acid in H_2O with the ratio 90:10. A mobile phase flow rate was 1 mL/min and the column temperature was controlled at 60 °C. A UV spectrometer was used as a detector and the absorbance of the eluate was measured at 195 mm.

3.7 References

Jabariyan, S. and Zanjanchi, M. A. (2012). A simple and fast sonication procedure to remove surfactant templates from mesoporous MCM-41. **Ultrasonics Sonochemistry**. 19: 1087-1093.

Khemthong, P., Prayoonpokarach, S., and Wittayakun, J. (2007). Synthesis and characterization of zeolite LSX from rice husk silica. **Suranaree Journal of Science and Technology**. 14(4): 367-379.

Kulawong, S., Prayoonpokarach, S., Neramittagapong, A., and Wittayakun, J. (2011). Mordenite modification and utilization as supports for iron catalyst in phenol hydroxylation. **Journal of Industrial and Engineering Chemistry**. 17: 346-351.

Rintramee, K., Föttinger, K., Rupprechter, G., and Wittayakun, J. (2012). Ethanol adsorption and oxidation on bimetallic catalysts containing platinum and base

metal oxide supported on MCM-41. **Applied Catalysis B: Environmental**. 115-116: 225-235.

Sanches-Silva, A., Rodr´ıguez-Bernaldo de Quirós, A., López-Hernández, J., and Paseiro-Losada, P. (2004). Comparison between high-performance liquid chromatography and gas chromatography methods for fatty acid identificationand quantification in potato crisps. **Journal of Chromatography A**. 1032: 7-15

Artkla, S., Grisdanurak, N., Neramittagapong, S., and Wittayakun., J., (2008). Characterization and catalytic performance on transesterification of palm olein of potassium oxide supported on RH-MCM-41 from rice husk silica. **Suranaree Journal of Science and Technology**. 15(2): 133-138
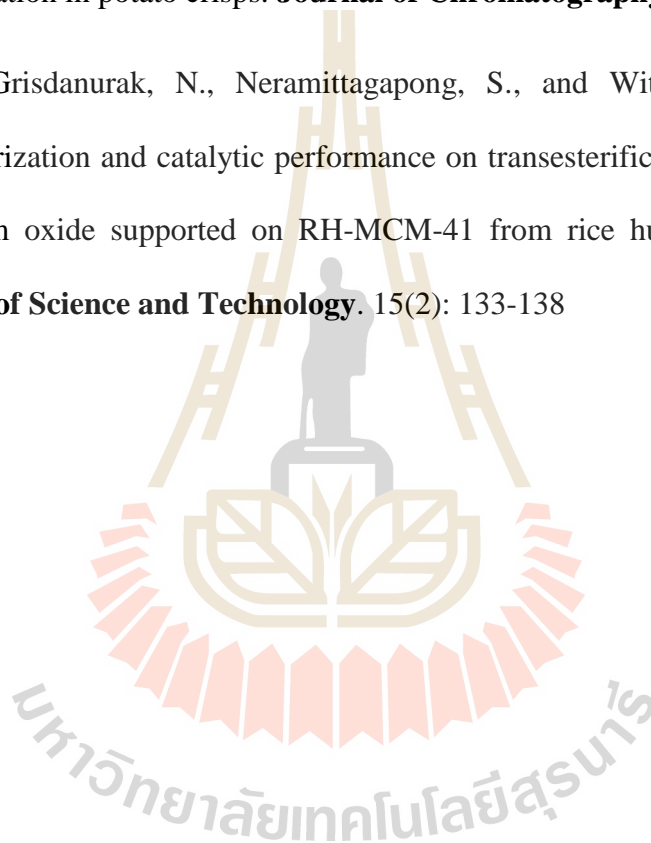
CHAPTER IV

RESULTS AND DISCUSSION

4.1 Characterization of adsorbents

4.1.1 XRD

Silica leached from rice husk was characterized by XRD to confirm the success of the extraction. The XRD pattern in Figure 4.1 shows a broad peak about 22° which is a characteristic of amorphous silica. The extracted silica was subsequently used as a silica source for the synthesis of MOR and MCM-41 and it was also used as the adsorbent.
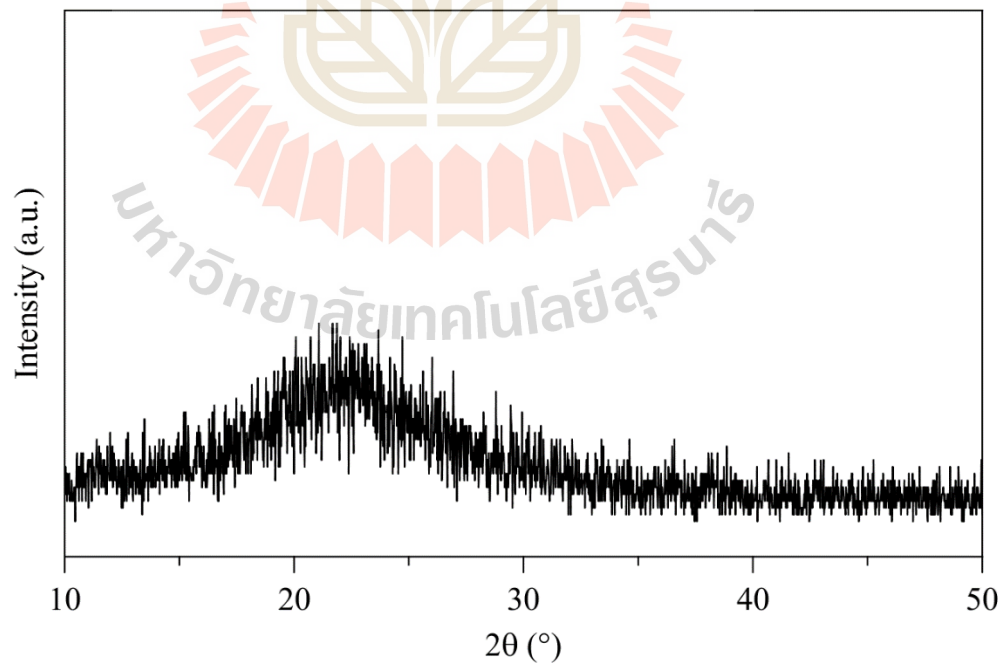
Figure 4.1 XRD pattern of silica.

MOR was successfully synthesized after 96 h of hydrothermal treatment and its XRD pattern is shown in Figure 4.2. All peaks are characteristic of MOR (Kulawong et al., 2011).

The X-ray patterns of the as-synthesized MCM-41 [MCM-41 (A)] and the calcined MCM-41 [MCM-41 (C)] at low angles between 2.50° and 7.00° are shown in Figure 4.3. For MCM-41 (A) characteristic peaks at 2.07° and weak peaks at 3.50°, 4.10° and 5.40° are the reflection of (100), (110), (200) and (210), respectively. The pattern demonstrated the hexagonal arranged channels (Bhagiyalakshmi et al., 2010). A similar pattern was also observed for MCM-41 (C); however, there is a small shift of the diffraction peaks toward higher 2θ. This is due to the lattice shrinkage as a result of the template removal by calcination (Kleitz et al., 2003). It is noted that lower intensity was obtained with MCM-41 (A). This is caused by the template filled in the mesopore structure (Goworek et al., 2007; Kleitz et al., 2001).
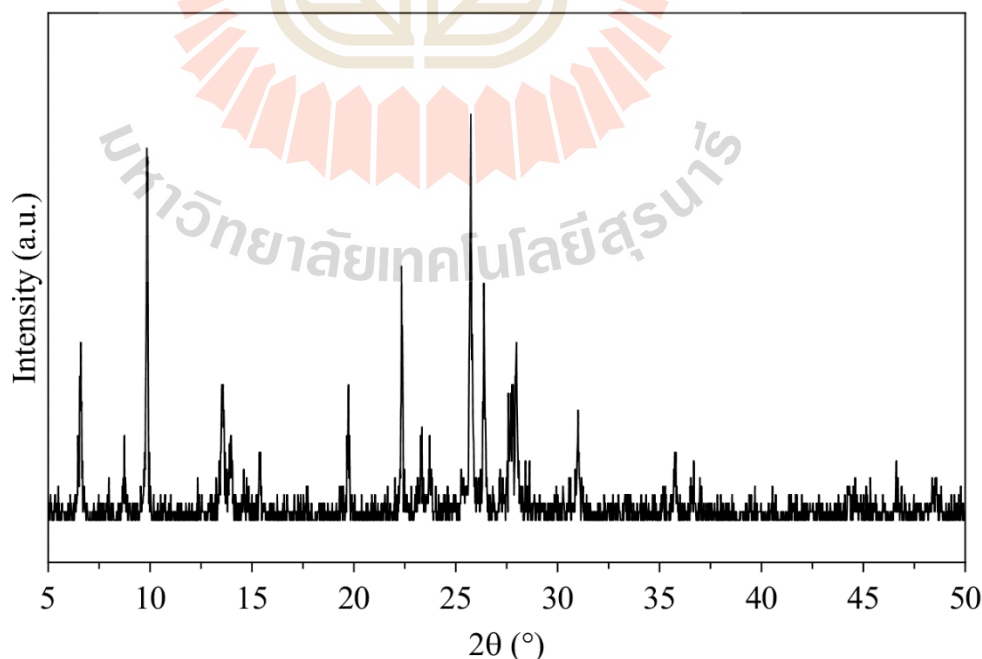
Figure 4.2 XRD pattern of MOR synthesized using rice husk as a silica source.
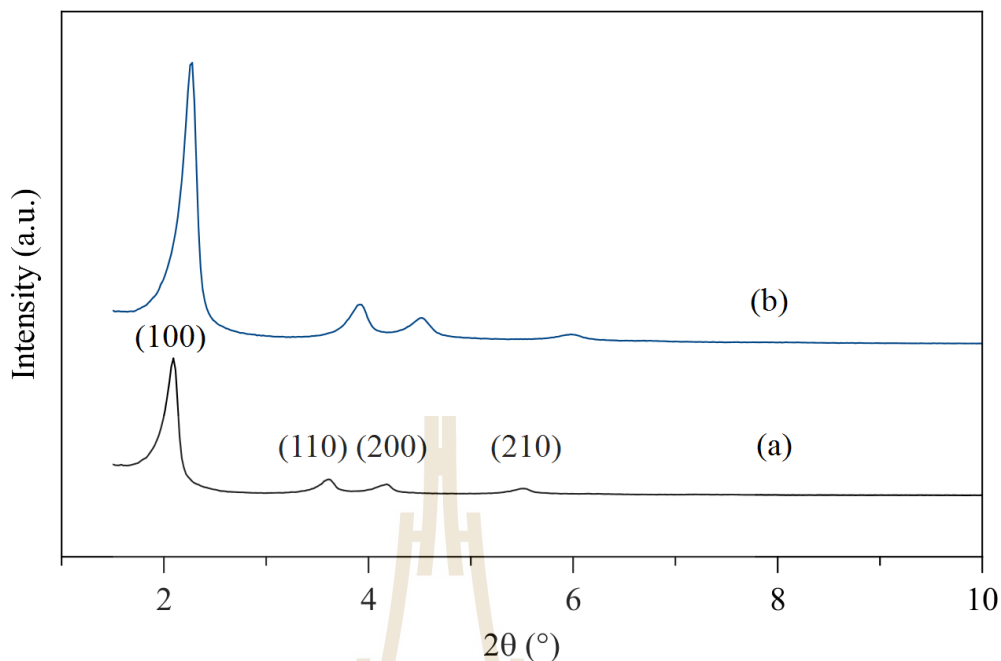
Figure 4.3 XRD patterns of (a) MCM-41 (A) and (b) MCM-41 (C).

4.1.2 Nitrogen adsorption-desorption analysis

The extracted silica from rice husk was subjected to nitrogen adsorption-desorption analysis to obtain its textual properties. Figure 4.4 shows a nitrogen adsorption-desorption isotherm of the silica which is of type IV. The material properties derived from the gas analysis are shown in Table 4.1.

The nitrogen adsorption-desorption isotherm of MOR is shown in Figure 4.5. It is a typical type I isotherm. The amount of adsorbed nitrogen increased rapidly at low relative pressure (P/P_0) and saturation was quickly reached. This is a characteristic of microporous materials. The textual properties of MOR are shown in Table 4.1.
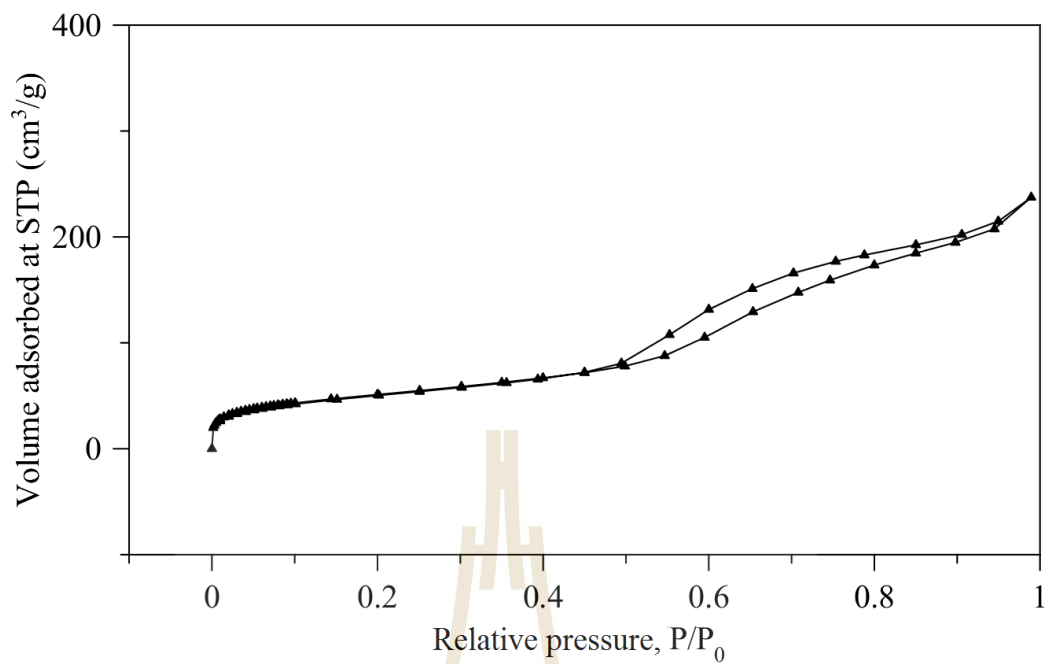
Figure 4.4 Nitrogen adsorption-desorption isotherm of the silica.
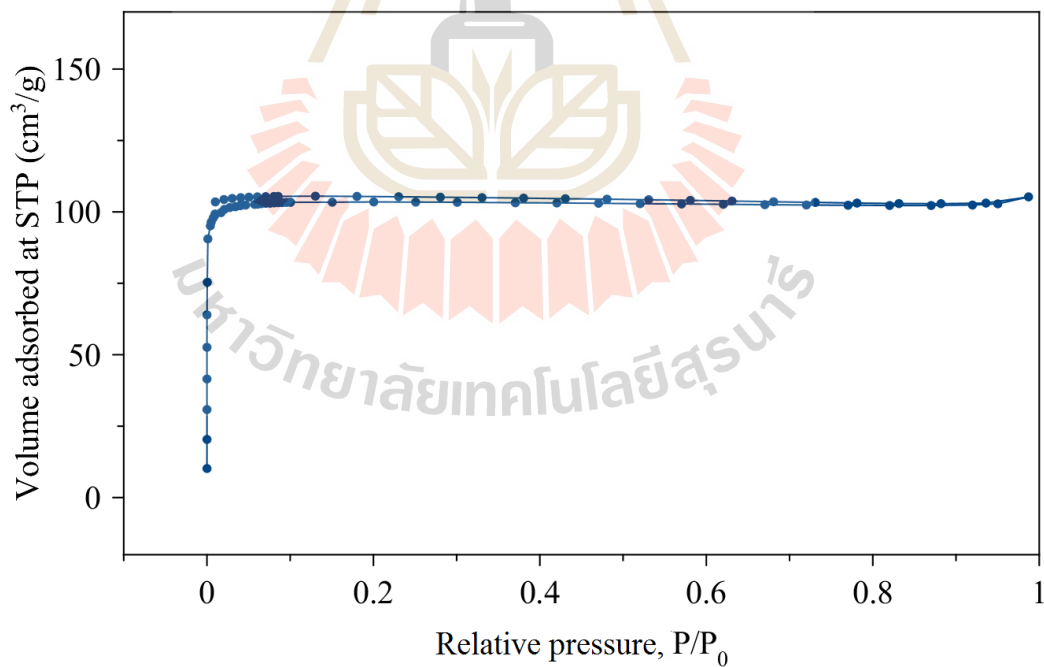
Figure 4.5 Nitrogen adsorption-desorption isotherm of MOR.

The nitrogen adsorption-desorption isotherms of MCM-41 (A) and MCM-41 (C) are shown in Figure 4.6. They are of the typical type IV according to the IUPAC classification. The MCM-41 (A) shows a small hysteresis loop at the P/P_0 range of 0.10-0.30. This could result from the weak interaction between nitrogen and the surfactant (Jaroniec et al., 1998). The values of the surface areas, specific pore volumes and average pore diameters are summarized in Table 4.1. The results show that the surface area and pore volume of MCM-41 (C) were increased after calcination because of the removal of the surfactant template.
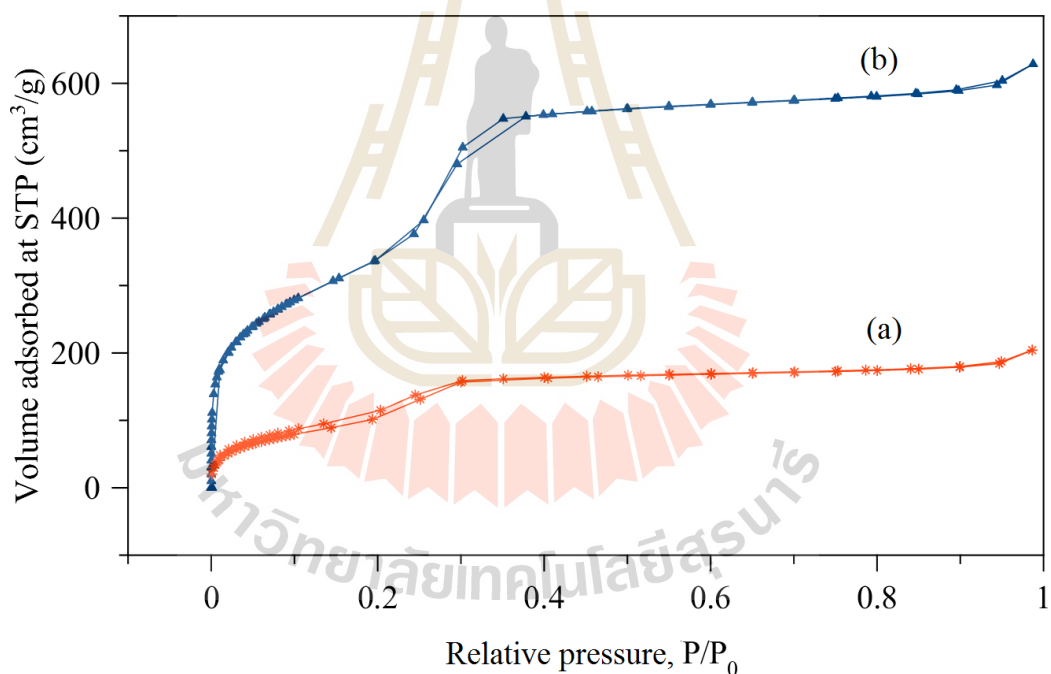
Figure 4.6 Nitrogen adsorption-desorption isotherms of (a) MCM-41 (A) and (b) MCM-41 (C).

Table 4.1 Results from nitrogen adsorption-desorption analysis.

Sample	BET surface area (m²/g)	Total pore volume (cm³/g)	Average pore diameter (Å)
Silica	181	0.367	81
MOR	339	0.159	19
MCM-41 (A)	434	0.316	29
MCM-41 (C)	1288	0.972	30

4.2 Adsorption study

4.2.1 Adsorption of oleic acid on silica, MOR, MCM-41 (A) and MCM-41 (C)

Adsorption of all adsorbents was initially compared by conducting adsorption experiments with various concentrations of oleic acid and a fixed amount of the adsorbents at 0.25 g. The temperature of solutions was controlled at 25 °C. The adsorption time was fixed at 1 h. The results are shown in Figure 4.7. The graph is plotted between the concentration of oleic acid in isooctane, X_e and the mass of oleic acid adsorbed per gram of the adsorbent or adsorption capacity, q_e.

All adsorbents can adsorb oleic acid and the adsorption capacity increases with the increasing of the concentration of oleic acid. The adsorption capacity tends to reach a plateau at high concentration of oleic acid.

Highest adsorption capacity is obtained with MCM-41 (C) and the adsorption capacities of MCM-41 (A) are slightly different from those of MCM-41 (C). High adsorption capacities in MCM-41 adsorbents could be due to the high surface area and the large pore diameter compared to the other adsorbents. The adsorption capacities of MOR and silica are about the same at high concentrations of the acid and about three
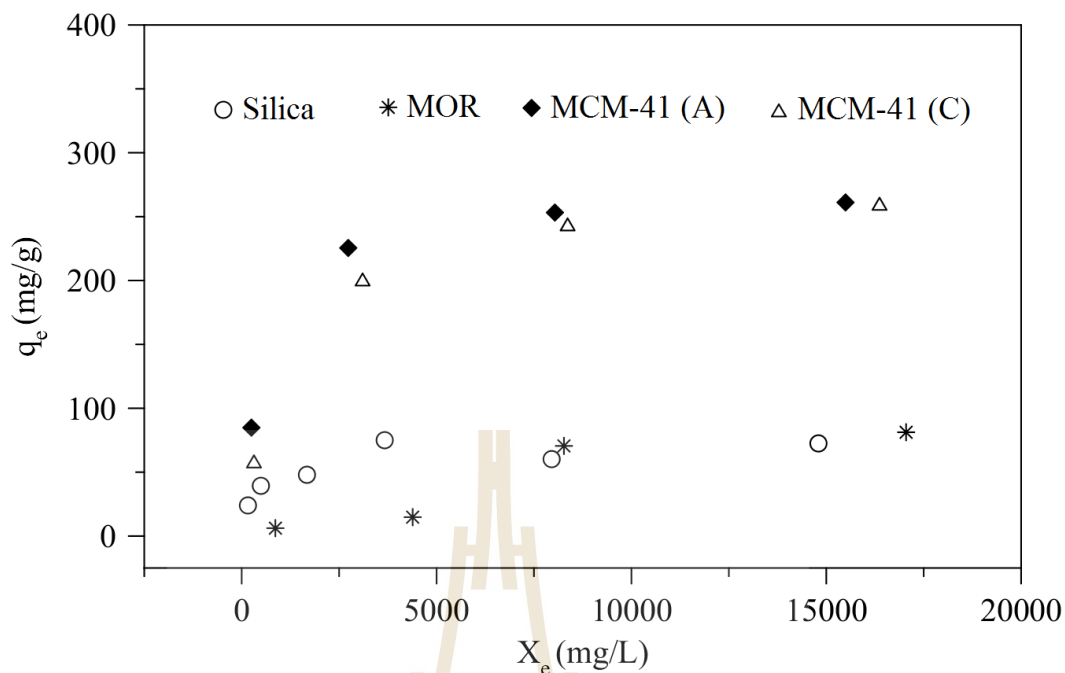
Figure 4.7 The adsorption capacities for oleic acid of silica, MOR and MCM-41 at various concentrations of oleic acid solutions.

times lower than those of the MCM-41 adsorbents. Although MOR has the surface area ~2 times higher than that of silica, silica has larger pore sizes that can accommodate the adsorption.

The adsorption of oleic acid proceeds via hydrogen bonding of the oxygen of the carboxyl group of the acid with the hydrogen of the silanol group. The hydrogen of the carboxyl group of the acid can also form a hydrogen bond with the oxygen of the silanol group (Atia et al., 2006).

The adsorption of oleic acid on the adsorbent surface can be verified through the IR spectroscopy. The IR spectra of the silica and the MOR before adsorption are shown in Figure 4.8 and 4.9, respectively. The bands in the range of 700-1200 cm^{-1} correspond to vibration modes of silica network where asymmetric stretching vibration

of the siloxane bond, Si-O-Si appears at 1109 cm^{-1} (Ahmed and Adam, 2007) and the broad band at 2800-3750 cm^{-1} is related to OH of the silanol group and water (Kalapathy et al., 2000; Yates et al., 1997). The bending vibration of Si-O-Si occurs at 450-460 cm^{-1} (Lenza and Vasconcelos, 2001). After the adsorption of oleic acid, the change of the spectrum due to H-bonding of the carboxyl group and the silanol group can be difficult to identify. However, the weak bands occurred at 2868 and 2942 cm^{-1} for silica and 2862 and 2939 cm^{-1} for MOR correspond to C-H stretching of the alkyl chain (Braga et al., 2011) which indicate the presence of oleic acid on the adsorbents.
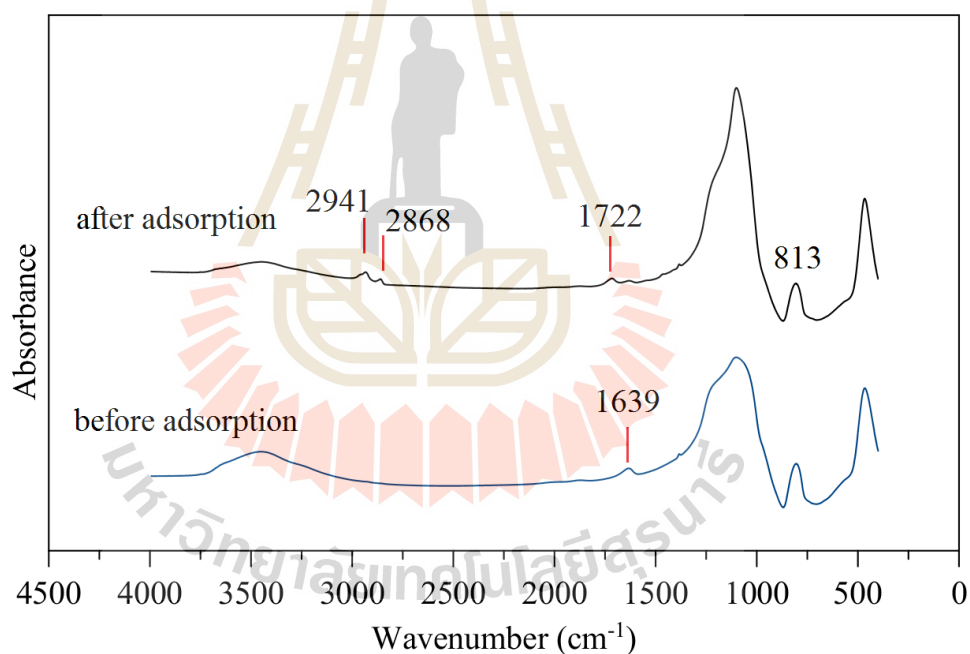
Figure 4.8 IR spectra of silica before and after the adsorption of oleic acid.
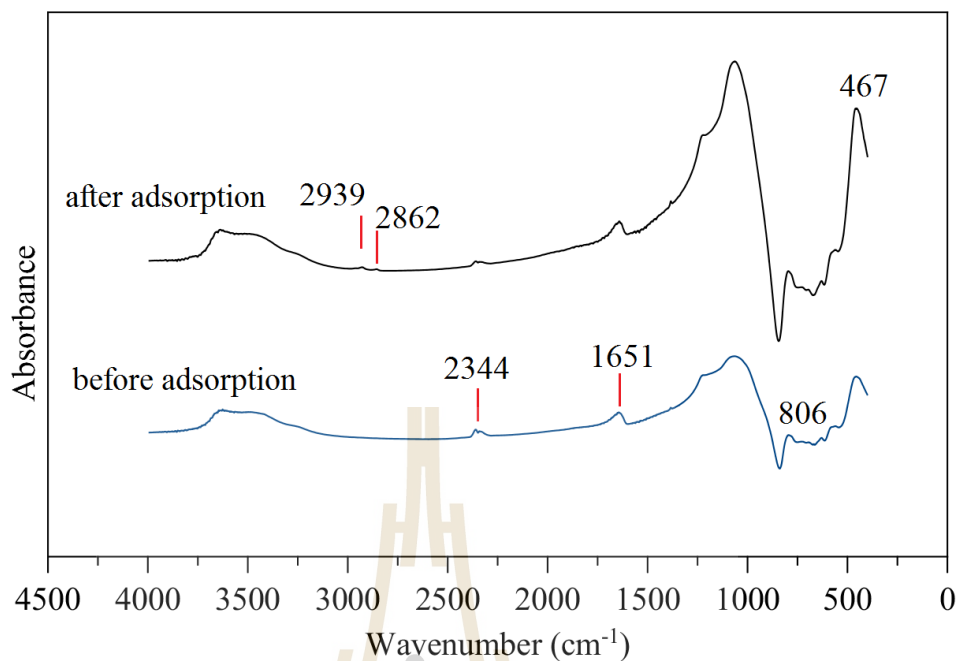
Figure 4.9 IR spectra of MOR before and after the adsorption of oleic acid.

The IR spectra of the MCM-41 (A) before adsorption in Figure 4.10 shows the band related to asymmetric Si-O-Si stretching at 1240 cm^{-1} and 1090 cm^{-1}, Si-O-Si bending vibration at 457 cm^{-1}, free silica at 804 cm^{-1}, C-H stretching modes at 2925 and 2858 cm^{-1} and C-H bending vibrations at 1480-1590 cm^{-1} that associate with the carbon long-chain template molecules (Braga et al., 2011).

For MCM-41 (A) after the adsorption of oleic acid, a weak band occurs at 1722 cm^{-1} and is assigned to C=O (Morais and Jardim, 2005) suggesting the presence of oleic acid on the adsorbent.

The spectra of MCM-41 (A) and MCM-41 (C) are shown in Figure 4.11. Characteristic bands of the Si-O-Si network are observed as in the silica and MOR. After calcination at 540 °C for 6 h, the bands related to the template molecules clearly disappear and the peak at 1643 cm^{-1} corresponds to vibration of molecular water

which is trapped in the silica framework (Appaturi et al., 2012; Lenza and Vasconcelos, 2001).
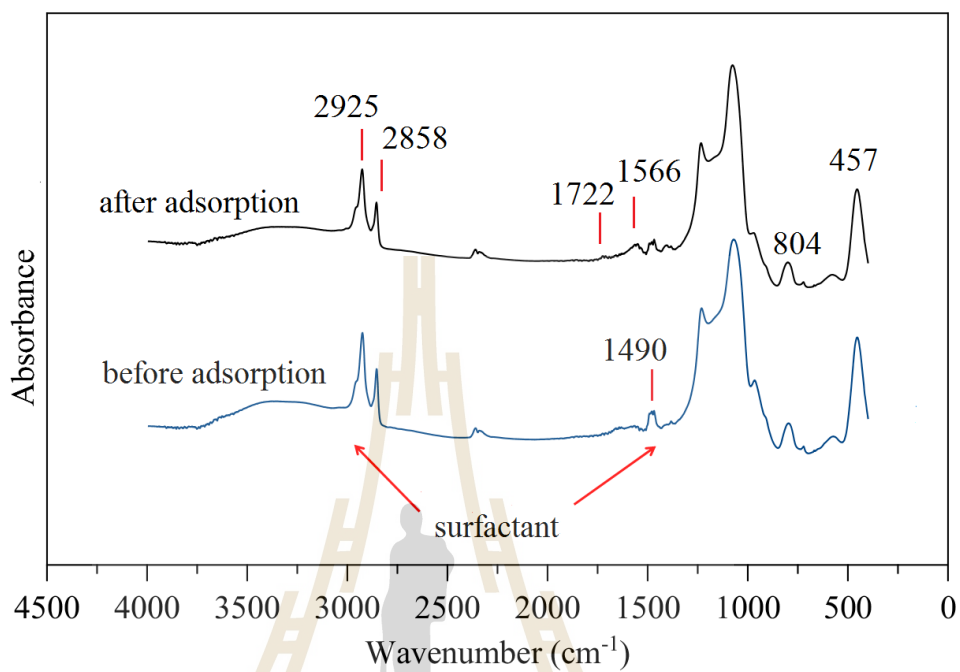
Figure 4.10 IR spectra of MCM-41 (A) before and after the adsorption of oleic acid.
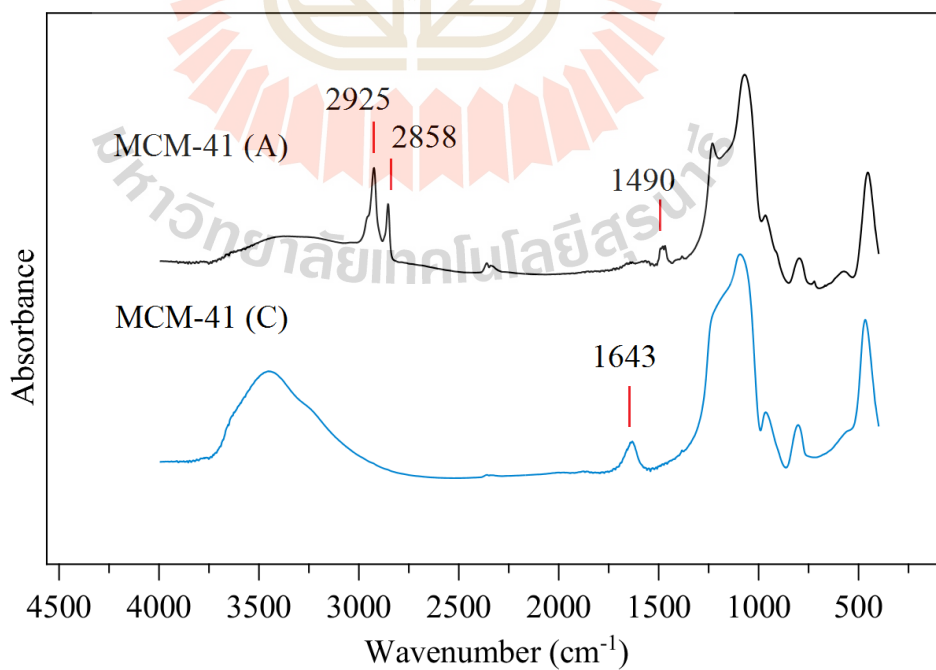
Figure 4.11 IR spectra of MCM-41 (A) and MCM-41 (C).

For MCM-41(C) after the adsorption, two bands appear at 2862 and 2933 cm^{-1} as shown in the Figure 4.12. The band at 2862 cm^{-1} could be assigned to CH_2 asymmetric vibrations and the other at 2933 cm^{-1} to CH_2 symmetric vibrations. The peak at 1710 cm^{-1} could be assigned to C=O stretching (Kumar et al., 2002; Lenza and Vasconcelos, 2001).

4.3 Equilibrium adsorption of MCM-41 (A) and MCM-41 (C)

From the adsorption capacity results in Figure 4.7, it is clear that MCM-41 (A) and MCM-41 (C) have relatively high adsorption capacities for oleic acid. Therefore, both adsorbents were used further for the equilibrium adsorption study.
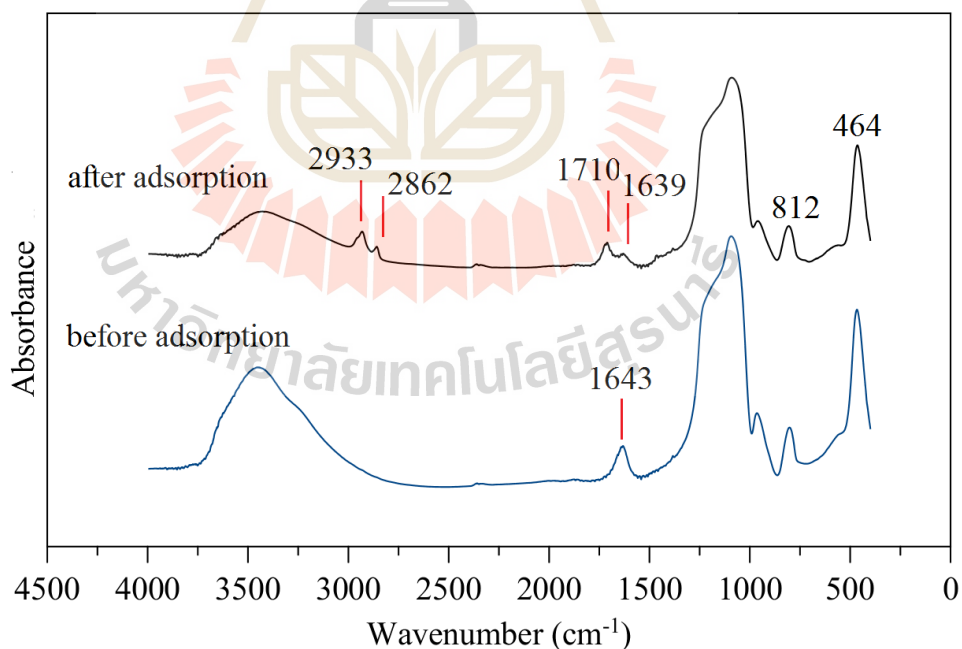
Figure 4.12 IR spectra of MCM-41 (C) before and after the adsorption of oleic acid.

To investigate the time that is used for the adsorption to reach the equilibrium, the adsorption study was carried out in solutions of 0.5% oleic acid with 0.25 g of the adsorbent. The adsorption time was varied in a range of 10-180 min. The temperature was controlled at 25 °C.

MCM-41 (A) adsorbs oleic acid rapidly and the adsorption capacity reaches the equilibrium in about 15 min as shown in Figure 4.13. Adsorption by MCM-41 (C) on the other hand is slower and the equilibrium is reached in 60 min. The MCM-41 (A) can adsorb oleic acid rapidly because the tail of CTAB having a hydrophobic character (Ghiaci et al., 2004) can interact with oleic acid and helps the diffusion of oleic inside the pore of MCM-41 (A). To make sure that the adsorption is at the equilibrium, the adsorption time of 60 min was used in further study.
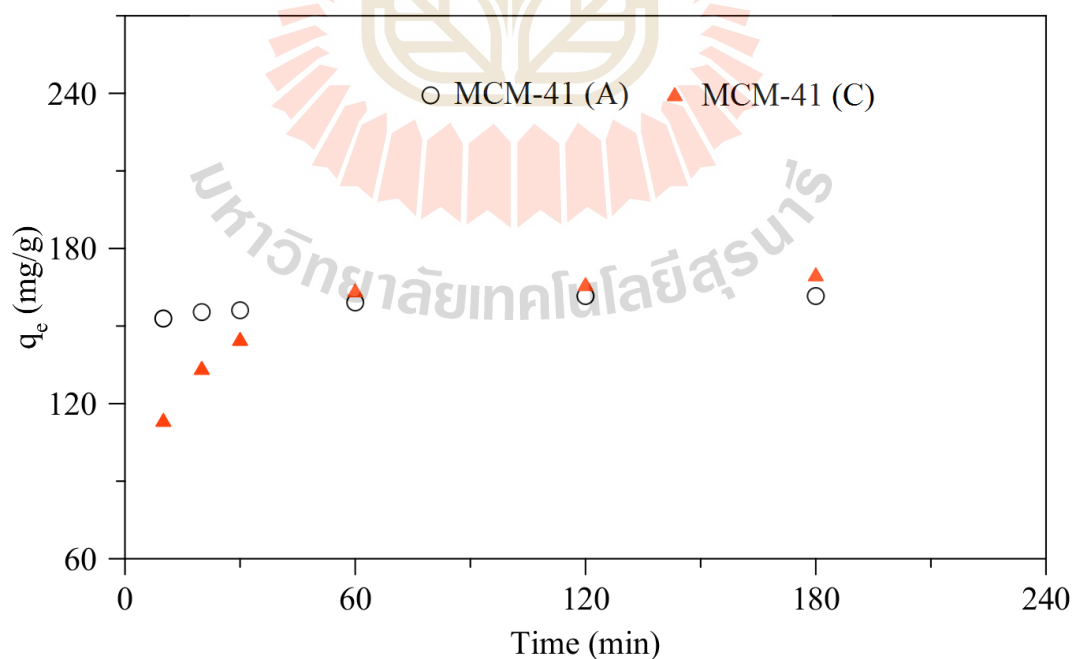
Figure 4.13 Time dependent adsorption for MCM-41 (A) and MCM-41 (C).

It was noted that the adsorption capacities of the MCM-41 (A) and MCM-41 (C) at equilibrium were about the same, ~160 mg/g although the surfactant still remained in the pore of the MCM-41 (A). Therefore, further investigation dealing with the sites of adsorption was conducted using nuclear magnetic resonance spectrometry (NMR).

Adsorption sites of MCM-41 (A) and MCM-41 (C) were investigated using ^{29}Si MAS-NMR spectroscopy. NMR spectra are shown in Figure 4.14 and 4.15. After the deconvolution of the NMR spectra, three peaks were obtained and can be used to calculate parameter such as condensation degree (Shylesh and Singh, 2006), relative proportion of different silicon environments (Costa et al., 2008) and molar percentage of silanol groups (Igarashi et al., 2003).

The chemical shifts of three peaks for both MCM-41 (A) and MCM-41 (C) are shown in Table 4.2. These chemical shifts are assigned to three silicon environments that are Q^2, two OH groups attach to the same silicon atom; Q^3, one free hydroxyl attaches to a silicon atom and Q^4, no OH group associates to the Si atom (Hamdan et al., 1997). Figure 4.16 shows the silicon environments of the aforementioned chemical shifts.

Table 4.2 ^{29}Si chemical shifts of the MCM-41 (A) and MCM-41 (C).

adsorbent	Q^2 (ppm); $Si(OSi)_2(OH)_2$	Q^3 (ppm); $Si(OSi)_3(OH)$	Q^4 (ppm); $Si(OSi)_4$
MCM-41 (A)	-92.0	-102.5	-112.3
MCM-41 (C)	-93.3	-103.0	-111.2
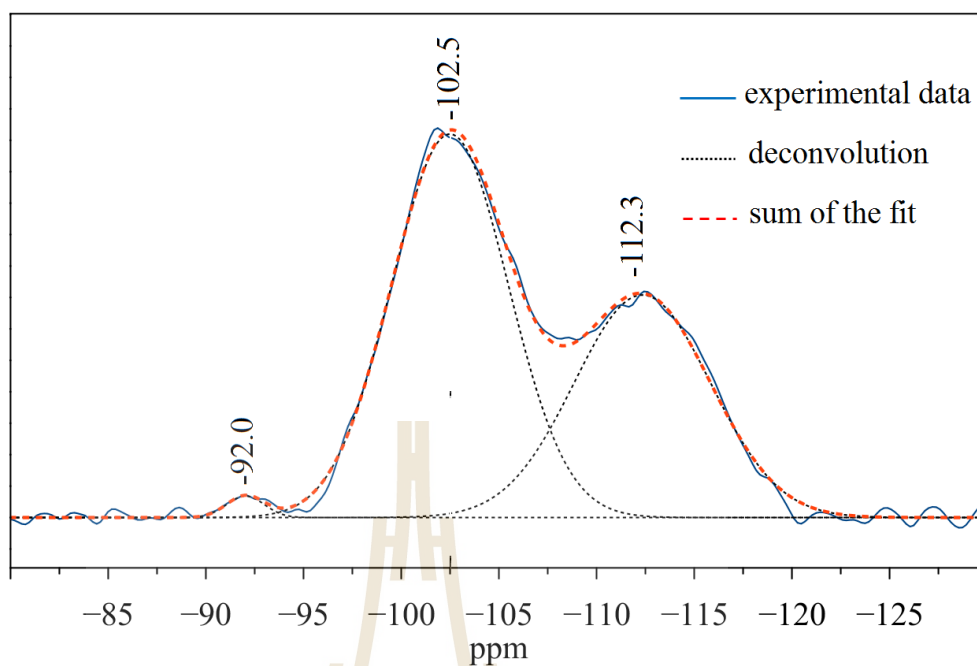
Figure 4.14 ^{29}Si MAS NMR spectrum of MCM-41 (A) and the deconvolution. The correlation coefficient of the fit is 0.9964.
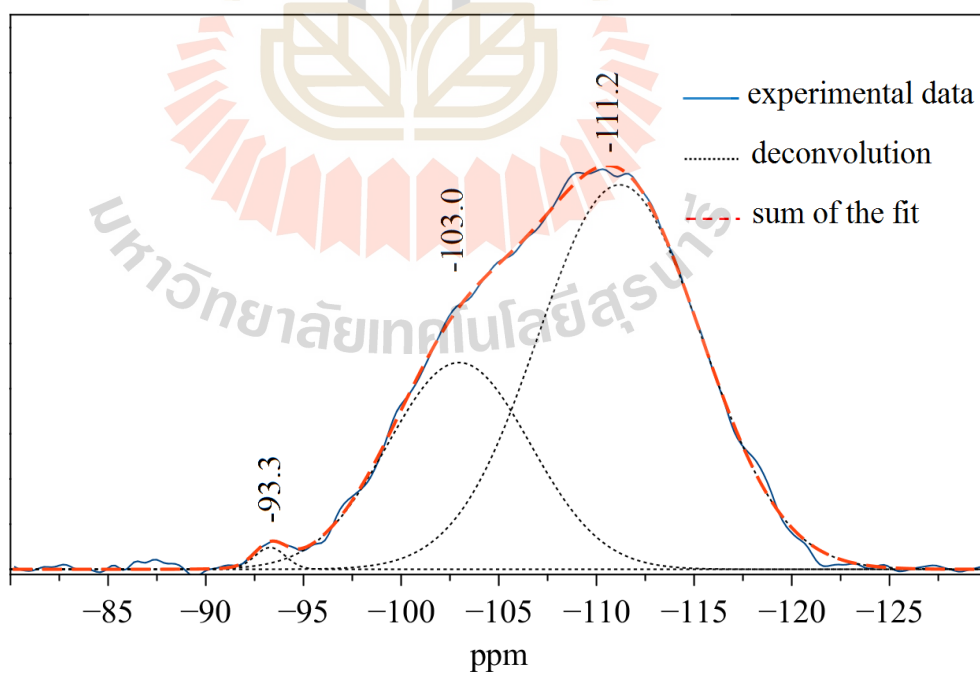
Figure 4.15 ^{29}Si MAS NMR spectrum of MCM-41 (A) and the deconvolution. The correlation coefficient of the fit is 0.9990.

$$Q^2 \qquad\qquad Q^3 \qquad\qquad Q^4$$

```
        H                       H                       Si
        |                       |                        |
        O                       O                        O
        |                       |                        |
 Si—O—Si—O—H             Si—O—Si—O—Si            Si—O—Si—O—Si
        |                       |                        |
        O                       O                        O
        |                       |                        |
        Si                      Si                       Si
```

(Geminal silanol or silanediols)   (Isolated silanols or single silanol)   (Siloxanes)
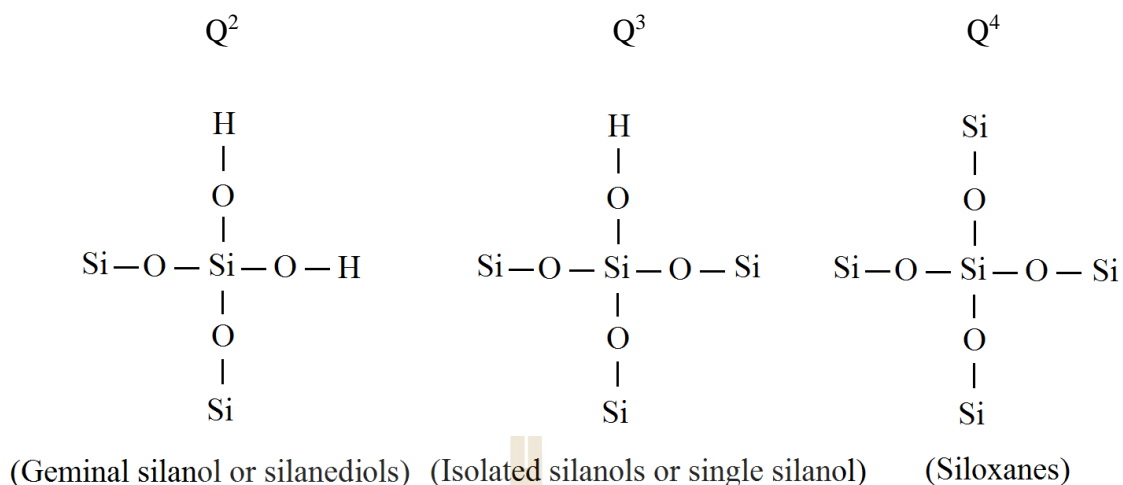
Figure 4.16 Chemical environments of silicon in silica surfaces (Costa et al., 2008; Shylesh and Sing, 2006).

From the deconvolution of the NMR spectra of MCM-41 (A) and MCM-41 (C), percentages of Q^2, Q^3 and Q^4 are obtained and shown in Table 4.3. When the template molecules were removed by calcination, the percent of Q^4 increased and that of Q^3 slightly decreased. This is due to the condensation of silanol group and the formation of siloxane bridge in the structure (Costa et al., 2008). According to the result in Table 4.3, the thermal treatment caused a slight decrease in the percentage of total silanol groups. This results conform well to the adsorption capacities of both MCM-41 adsorbents that are about the same.

58

Table 4.3 Relative proportions of the different silicon chemical environments determined by ^{29}Si MAS-NMR.

Adsorbent	Relative proportion of the chemical environment (%)			SiOH (mol %-Si)[a]
	Q^2	Q^3	Q^4	
MCM-41 (A)	1.1	59.0	39.9	61.2
MCM-41 (C)	0.7	31.7	67.6	33.1

[a]Relative amount of silanol groups = $[(2Q^2 + Q^3)/ (Q^2 + Q^3 + Q^4)] \times 100\%$ (Igarashi et al., 2003)

4.4 Isotherm study

An adsorption isotherm describes the relationship between the adsorption capacity and the remaining amount of an adsorbate in a solution and is the method used to evaluate the mechanism of adsorption. The experimental equilibrium data of this study are correlated with the Langmuir and Freundlich model. The data used for fitting with the models were from the adsorption studies using 0.25 g of the adsorbent mixed in a solution of oleic acid which the concentration was within the range of 0.25-3.00%. The adsorption time was fixed at 1 h. The adsorption temperature was varied in a range of 25-50 °C.

4.4.1 MOR

The adsorption data from the study with MOR were fitted with Langmuir and Freundlich model and the results are shown in Table 4.4 and 4.5. MOR has relative low adsorption capacity for oleic acid. For Langmuir model, the data were used for the plot of X_e/q versus X_e. The correlation coefficients (R^2) for every studied temperatures were

less than 0.9 indicating that the adsorption of oleic acid on MOR does not follow Langmuir model.

Table 4.5 shows the Freundlich parameters for oleic acid adsorption onto MOR that can be examined from the plots of ln q_e versus ln X_e in the temperature range of 25-40 °C. The correlation coefficients were > 0.9 at 25 and 40 °C and about 0.8 at 30 °C. Although Freundlich model is not the best fitted model for the experimental data, it can be inferred that the adsorption sites are not uniform.

Table 4.4 Langmuir isotherm models, Langmuir constants and other derived parameters for the adsorption of oleic acid onto MOR.

Temperature (°C)	Linear equation[a]	R^2	q_m (mg/g)	K_A (L/mg)
25	y = 0.0011x + 182.9993	0.0024	909.1	6.01×10^{-6}
30	y = 0.0144x + 90.7236	0.7458	69.4	1.59×10^{-4}
40	y = -0.0036x + 301.1958	0.1193	212.8	-1.20×10^{-5}

[a] A linear form of Langmuir model is $\dfrac{X_e}{q} = \dfrac{X_e}{q_m} + \dfrac{1}{K_A q_m}$.

Table 4.5 Freundlich isotherm models, Freundlich constants and other derived parameters for the adsorption of oleic acid onto MOR.

Temperature (°C)	Linear equation[a]	R^2	1/n	K_F (mg/g)
25	y = 0.9187x – 4.5035	0.9228	0.0187	1.11×10^{-2}
30	y = 0.4373x – 0.3466	0.7948	0.4373	7.07×10^{-2}
40	y = 1.1775x – 7.0988	0.9189	1.1775	8.00×10^{-3}

[a] A linear form of Freundlich model is $\ln q = \ln K_F + \dfrac{1}{n} \ln X_e$.

4.4.2 MCM-41 adsorbents

The linear form of the Langmuir plot for adsorption of oleic acid onto MCM-41 (A) and MCM-41 (C) can be examined from the plots of X_e/q versus X_e in the temperature range of 25-50 °C. Table 4.6 and 4.7 show the Langmuir isotherm equations and derived parameters. The R^2 value of > 0.99 indicates that the adsorption data of oleic acid onto both MCM-41 adsorbents were fitted well with the Langmuir isotherm within the concentration range used in this experiment.

Comparing q_m values for both adsorbents at the same adsorption temperature, the values are about the same at 25 and 35 °C, but slightly different at 40 and 50 °C. Adsorption capacity for both adsorbents tend to be about the same. This could be due to that the adsorption could take place only about the entrance of the pores. For MCM-41 (C) the adsorbed acid molecules could hinder further adsorption of the acid inside the pores. Whereas for MCM-41 (A), CTAB inside the pores of MCM-41 could block the acid adsorption inside the pores.

The fitted isotherm curves along with the experimental data are shown in Figure 4.17 and 4.18. The experimental data distributed closely to the model line at 25 °C, 30 °C, 40 °C and 50 °C indicating a good agreement of the experimental data and the fitted model. The adsorption of oleic acid onto MCM-41 (A) and MCM-41 (C) is influenced by temperature, that is the adsorption capacity decreases with the increasing temperature. This suggests that the adsorption of oleic acid on MCM-41 adsorbents is an exothermic process.

Table 4.6 Langmuir isotherm equations, Langmuir constants and other derived parameters for the adsorption of oleic acid onto MCM-41 (A).

Temperature (°C)	Linear equation	R^2	q_m (mg/g)	K_A (L/mg)
25	y = 0.0036x + 4.4041	0.9951	277.8	8.17×10^{-4}
30	y = 0.0039x + 2.0501	0.9946	256.7	1.90×10^{-3}
40	y = 0.0047x + 2.8752	0.9904	212.8	1.64×10^{-3}
50	y = 0.0050x + 3.1015	0.9860	200.0	1.61×10^{-3}

Table 4.7 Langmuir isotherm equations, Langmuir constants and other derived parameters for the adsorption of oleic acid onto MCM-41 (C).

Temperature (°C)	Linear equation	R^2	q_m (mg/g)	K_A (L/mg)
25	y = 0.0037x + 2.0100	0.9972	270.3	1.84×10^{-3}
30	y = 0.0039x + 2.0286	0.9949	256.4	1.92×10^{-3}
40	y = 0.0041x + 1.9384	0.9951	243.9	2.12×10^{-3}
50	y = 0.0062x + 1.6319	0.9940	161.3	3.80×10^{-3}
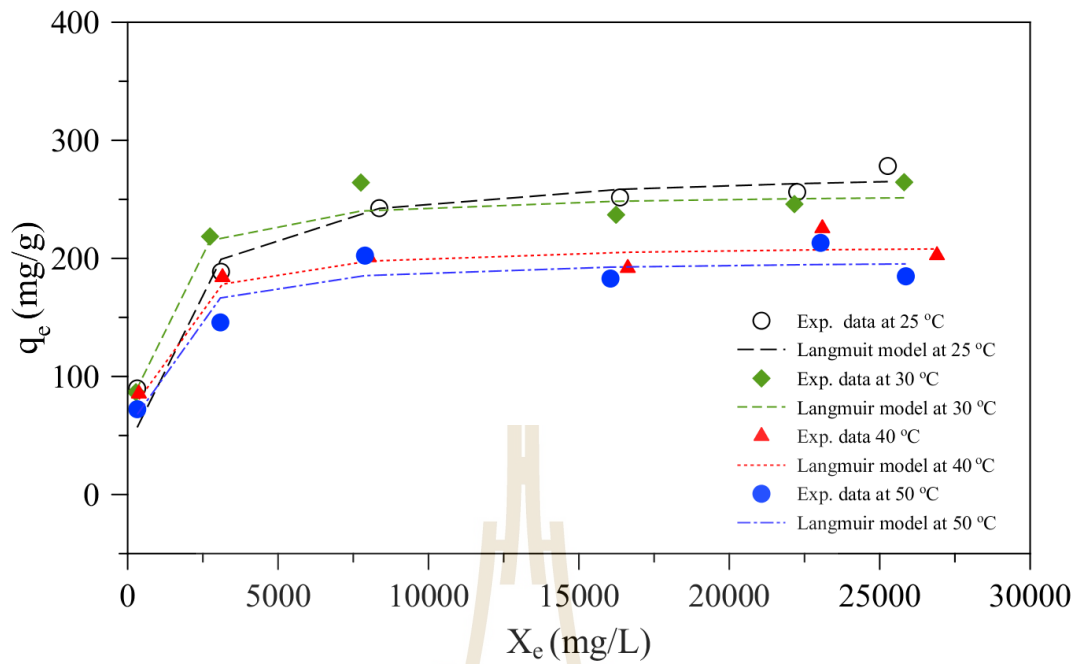
Figure 4.17 Langmuir isotherm models and the experimental data of the adsorption study using MCM-41 (A) at various temperatures.
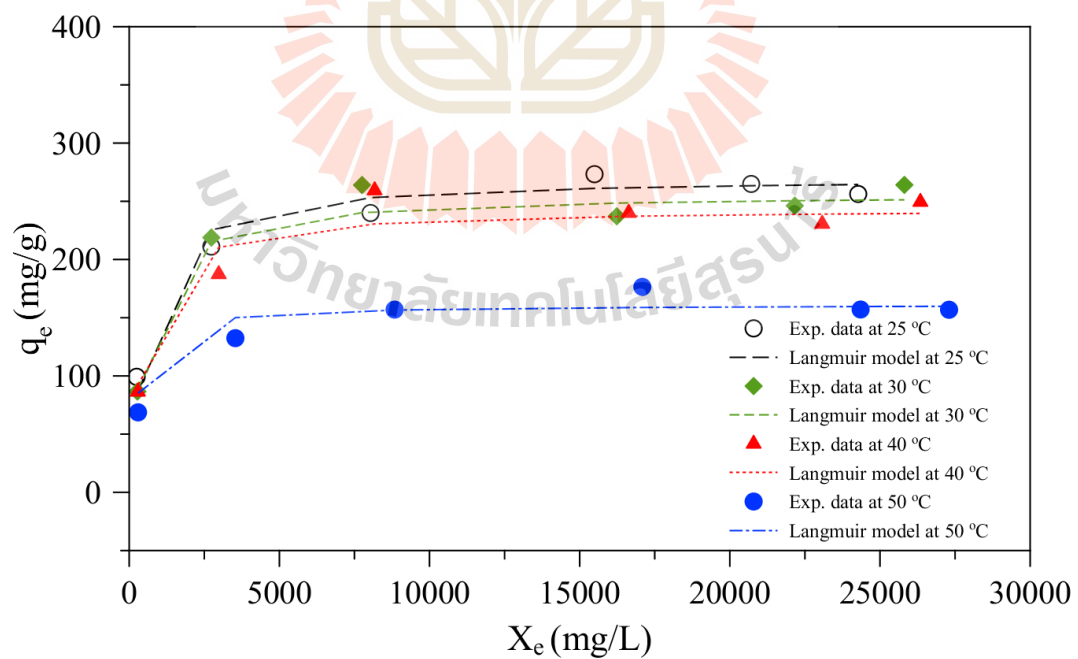
Figure 4.18 Langmuir isotherm models and the experimental data of the adsorption study using MCM-41 (C) at various temperatures.

Other important factor derived from the Langmuir isotherm is the dimensionless constant separation factor, R_L. The value of R_L are summarized in Table 4.8 and 4.9. The value in the range 0-1 indicates that the equilibrium adsorption is favorable at the temperature studied (Adam and Chua, 2004; Dada et al., 2012).

The adsorption data were also correlated to Freundlich isotherm model. The linear form of the Freundlich model for adsorption of oleic acid onto MCM-41 adsorbents can be examined from the plots of $\ln q_e$ versus $\ln X_e$ in the temperature range of 25-50 °C and the results are shown in Table 4.10 and 4.11. The values of R^2 indicate that the adsorption of oleic acid onto the MCM-41 adsorbents does not fit well with the Freundlich isotherm.

Table 4.8 The constant separation factors for the adsorption of oleic acid onto MCM-41 (A) at various initial acid concentrations and temperatures.

Initial concentration (%)	R_L at temperature			
	25 °C	30 °C	40 °C	50 °C
0.10	0.5019	0.3156	0.3324	0.3731
0.50	0.1969	0.0964	0.1091	0.1201
1.00	0.1018	0.0481	0.0575	0.0589
2.00	0.0608	0.0275	0.0319	0.0335
2.50	0.0470	0.0209	0.0236	0.0241
3.00	0.0418	0.0181	0.0207	0.0219

Table 4.9 The constant separation factors for the adsorption of oleic acid onto MCM-41 (C) at various initial acid concentrations and temperatures.

Initial concentration (%)	R_L at temperature			
	25 °C	30 °C	40 °C	50 °C
0.10	0.3042	0.3133	0.2907	0.2114
0.50	0.1008	0.0955	0.0887	0.0514
1.00	0.0495	0.0476	0.0421	0.0247
2.00	0.0289	0.0272	0.0242	0.0138
2.50	0.0227	0.0207	0.0183	0.0101
3.00	0.3042	0.3133	0.2907	0.2114

Table 4.10 Freundlich isotherm models, Freundlich constants and other derived parameters for the adsorption of oleic acid onto MCM-41 (A).

Temperature (°C)	Linear equation	R^2	1/n	K_F (mg/g)
25	y = 0.2488x + 3.1381	0.9611	0.2488	23.06
30	y = 0.2279x + 3.3409	0.8406	0.2279	28.24
40	y = 0.2009x + 3.3864	0.8486	0.2009	29.56
50	y = 0.2280x + 3.0595	0.8933	0.2280	21.32

Table 4.11 Freundlich isotherm models, Freundlich constants and other derived parameters for the adsorption of oleic acid onto MCM-41 (C).

Temperature (°C)	Linear equation	R^2	1/n	K_F (mg/g)
25	y = 0.2127x + 3.5142	0.9289	0.2127	33.59
30	y = 0.2278x + 3.3423	0.8402	0.2278	28.28
40	y = 0.2285x + 3.2776	0.8822	0.2285	26.51
50	y = 0.1911x + 3.2213	0.9036	0.1911	25.06

4.5 Thermodynamic parameters

From the adsorption data conducted at different temperatures, enthalpy change (ΔH) and entropy change (ΔS) for the adsorption can be calculated from the slope and intercept of a graph plotting between $\ln K_D$ versus $1/T$ as shown in Figure 4.19 and 4.20. The results are given in Table 4.12. The negative values of ΔH suggest that the adsorption is an exothermic process.

The ΔS is related to variations of the order-disorder in a system. The positive values of ΔS for the adsorption with both adsorbents suggest that the adsorption system was in a higher state of disorder at the equilibrium (Adam and Chua, 2004).

For Gibb free energy change (ΔG) the values were obtained from equation $\Delta G = \Delta H - T\Delta S$ and are shown in Table 4.12. The negative values of ΔG indicate that the adsorption of the acid on both adsorbents is spontaneous (Gupta et al., 2004).
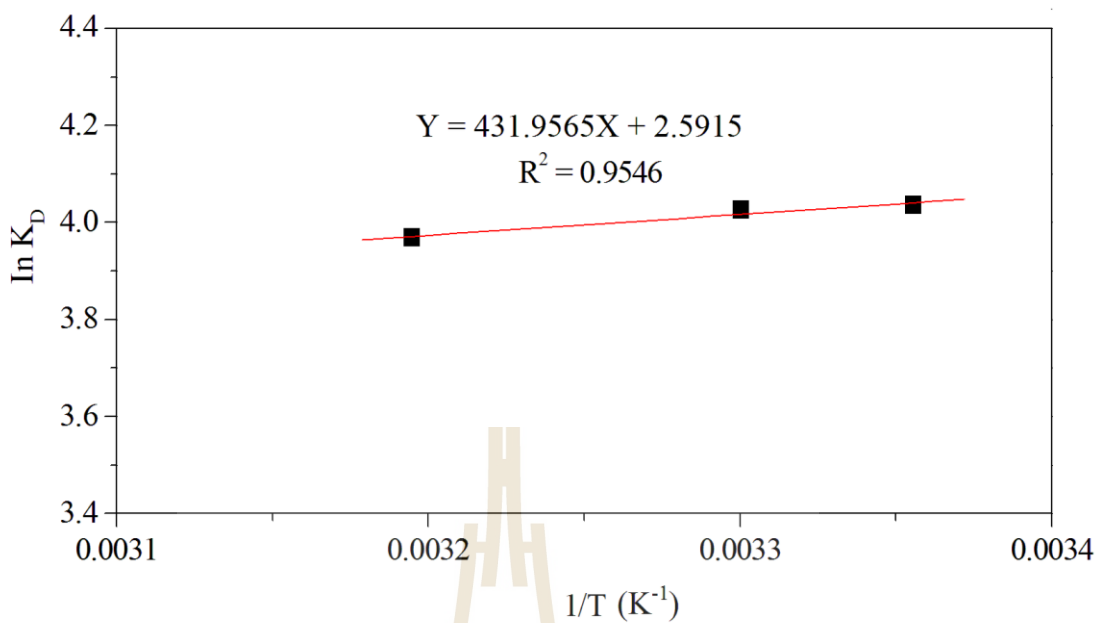
Figure 4.19 The plot of ln K_D versus 1/T for the adsorption of oleic acid with MCM-41 (A). Condition: adsorption time; 60 min, the acid concentration; 118 mg/ 25 mL, the amount of adsorbent; 0.25 g/ 25 mL.
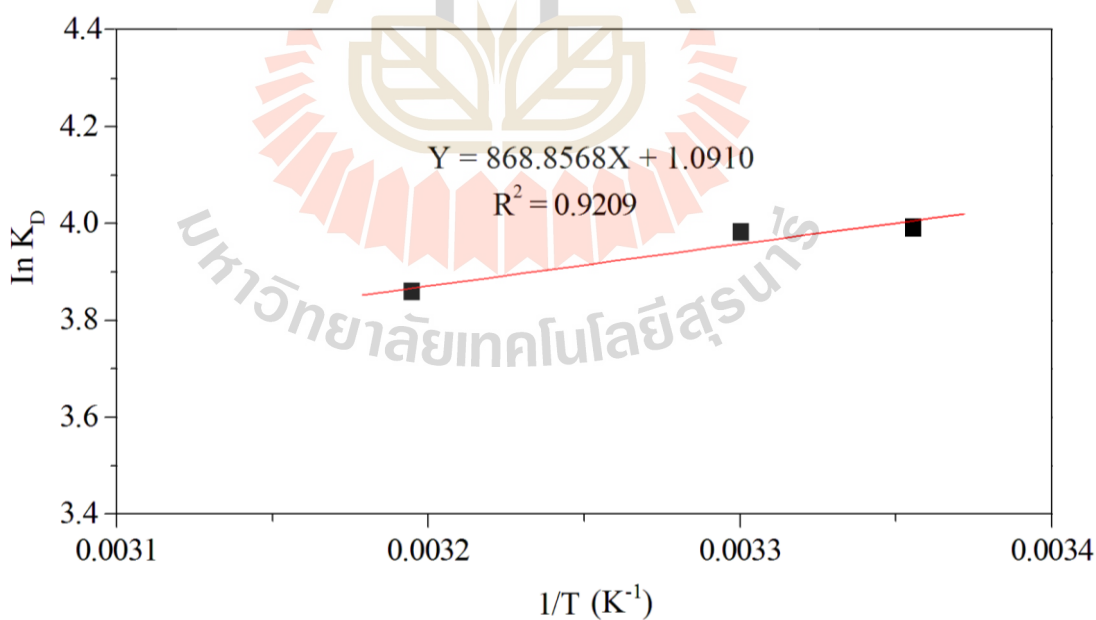
Figure 4.20 The plot of ln K_D versus 1/T for the adsorption of oleic acid with MCM-41 C). Condition: adsorption time; 60 min, the acid concentration; 118 mg/ 25 mL, the amount of adsorbent; 0.25 g/ 25 mL.

Table 4.12 Thermodynamic parameters for the adsorption of oleic acid onto MCM-41 (A) and MCM-41 (C).

Adsorbent	ΔH (kJ/mol)	ΔS (J/mol)	ΔG (kJ/mol)		
			25 °C	30 °C	40 °C
MCM-41 (A)	-3.59	21.5	-10.01	-10.12	-10.34
MCM-41 (C)	-7.22	9.07	-9.93	-9.97	-10.06

4.6 Adsorption of FFA in soybean oil

Both MCM-41 (A) and MCM-41 (C) were used for the adsorption of 1.0% oleic acid in soybean oil. The mixture of the adsorbent and the acid solution was stirred for 60 min at 25 °C. After that the adsorbent was removed by centrifugation and the amount of the acid in the solution was determined. The results are shown in Table 4.13. The adsorption capacity of MCM-41 (A) was 178.7 mg/g which was lower than that of the adsorption conducted in isooctane, $q_e = 242.5$ mg/g, with the same concentration of oleic acid and adsorption temperature. For MCM-41 (C), the adsorption of the acid was not observed. This could be due to that triacylglycerol could also be adsorbed on the adsorbents via hydrogen bonding of carbonyl group to silanol group (Yates et al., 1997). Because of the bulky structure of the triacylglycerol once adsorbed it could hinder the adsorption of oleic acid on both adsorbents.

Table 4.13 The adsorption capacities of MCM-41 (A) and MCM-41 (C) in soybean oil.

Adsorbent	q_e (mg/g)	% removal
MCM-41 (A)	178.7	16.2
MCM-41 (C)	no adsorption	-

4.7 References

Adam, F. and Chua, J. H. (2004). The adsorption of palmytic acid on rice husk ash chemically modified Al (III) ion using the sol-gel technique. **Journal of Colloid and Interface Science**. 280: 55-61.

Ahmed, A. E. and Adam, F. (2007). Indium incorporated silica from rice husk and its catalytic activity. **Microporous and Mesoporous Materials**. 103: 284-295.

Appaturi, J. N., Adam, F., and Khanam, Z. (2012). A comparative study of the regioselective ring opening of styrene oxide with aniline over several types of mesoporous silica materials. **Microporous and Mesoporous Materials**. 156: 16-21.

Atia, A. A., El-Nahas, A. M., Marie, A. M., and Al Mahdy, L. D. (2006). Adsorption of oleic acid on silica gel derived from rice ash hulls: Experimental and theoretical studies. **Adsorption Science and Technology**. 24(9): 797-814.

Bhagiyalakshmi, M., Yun, L. J., Anuradha, R., and Jang, H. T. (2010). Synthesis of chloropropylamine grafted mesoporous MCM-41, MCM-48 and SBA-15 from

rice husk ash: their application to CO_2 chemisorption. **Journal of Porous Materials**. 17: 475-484.

Braga, P. R. S., Costa, A. A., de Macedo, J. L., Ghesti, G. F., de Douza, M. P., Dias, A. J., and Dias, S. C. L. (2011). Liquid phase calorimetric-adsorption analysis of Si-MCM-41: Evidence of strong hydrogen-bonding sites. **Microporous and Mesoporous Materials**. 139: 74-80.

Costa, A. A., Ghesti, F. G., de Macedo, J. L., Braga, V. S., Santos, M. M., Dias, J. A., and Dias, S. C. L. (2008). Immobilization of Fe, Mn and Co tetraphenylporphyrin complexes in MCM-41 and their catalytic activity in cyclohexene oxidation reaction by hydrogen peroxide. **Journal of Molecular Catalysis A: Chemical**. 282: 149-157.

Dada, A.O., Olalekan, A.P., Olatunya, A.M., DaDa, O. (2012). Langmuir, Freundlich, Temkin and Dubinin-Radushkevich isotherms studies of equilibrium sorption of Zn^{2+} onto phosphoric acid modified rice husk. **Journal of Applied Chemistry**. 3(1): 38-45.

Ghiaci, M., Abbaspur, A., Kai, R., and Seyedeyn-Azad, F. (2004). Equilibrium isotherm studies for the sorption of benzene, toluene, and phenol onto organo-zeolites and as-synthesized MCM-41. **Separation and Purification Technology**. 40: 217-229.

Goworek, J., Kierys, A., and Kusak, R. (2007). Isothemal template removal from MCM-41 in hydrogen flow. **Microporous and Mesoporous Materials**. 98: 242-248.

Grün, M., Unger, K. K., Matsumoto, A., and Tsutsumi, K. (1999). Novel pathways for the preparation of mesoporous MCM-41 materials: Control of porosity and morphology. **Microporous and Mesoporous Materials**. 27: 207-216.

Gupta, V. K., Singh, P., and Rahman, N. (2004). Adsorption behavior of Hg(II), Pb(II), and Cd(II) from aqueous solution on Duolite C-433: a synthetic resin. **Journal of Colloid and Interface Science**. 275: 398-402.

Hamdan, H., Muhid, M. N. M., Endud, S., Listiorini, E., and Ramli, Z. (1997). ^{29}Si MAS NMR, XRD and FESEM studies of rice husk silica for the synthesis of zeolites. **Journal of Non-Crystalline Solids**. 211: 126-131.

Igarashi, N., Koyano, K. A., Tanaka, Y., Nakata, S., Hashimoto, K., and Tatsumi, T. (2003). Investigation of the factors influencing the structural stability of mesoporous silica molecular sieves. **Microporous and Mesoporous Materials**. 59: 43-52.

Jaroniec, C. P., Kruk, M., and Jaroniec, M. (1998). Tailoring surface and structural properties of MCM-41 silicas by bonding organosilanes. **The Journal of Physical Chemistry**. 102: 5503-5510.

Kalapathy, U. and Proctor, A. (2000). A new method for free fatty acid reduction in frying oil using silicate films produced from rice hull ash. **Journal of the American Oil Chemists' Society**. 77(6): 593-598.

Kleitz, F., Schmidt, W., and Schüth, F. (2001). Evolution of mesoporous materials during the calcinations process: structural and chemical behavior. **Microporous and Mesoporous Materials**. 44-45: 95-109.

Kleitz, F., Schmidt, W., and Schüth, F. (2003). Calcination behavior of different surfactant-templated mesostrured silica materials. **Microporous and Mesoporous Materials**. 65: 1-29.

Kumar, T. V. V., Prabhakar, S., and Raju, G. B. (2002). Adsorption of oleic acid at sillimanite/water interface. **Journal of Colloid and Interface Science**. 247: 275-281.

Kulawong, S., Prayoonpokarach, S., Neramittagapong, A., and Wittayakun, J. (2011). Mordenite modification and utilization as supports for iron catalyst in phenol hydroxylation. **Journal of Industrial and Engineering Chemistry**. 17: 346-351.

Lenza, R. F. S. and Vasconcelos, W. L. (2001). Preparation of silica by sol-gel method using formamide. **Materials Research**. 4(3): 189-194.

Morais, L. S. R. and Jardim, L. C. S. F. (2005). Characterization of a new stationary phase based on microwave immobilized polybutadiene on titanium oxide-modified silica. **Journal of Chromatography A**. 1073: 127-135.

Shylesh, S. and Singh, A. P. (2006). Heterogenized vanadyl cations over modified silica surfaces. **Journal of Catalysis**. 244: 52-64.

Yates, R. A., Caldwell, J. D., and Perkins, E. G. (1997). Diffuse reflectance fourier transform infrared spectroscopy of triacylglycerol and oleic acid adsorption on synthetic magnesium silicate. **Journal of the American Oil Chemists' Society**. 74: 289-292.

CHAPTER V

CONCLUSION

This research focused on the removal of oleic acid in isooctane solutions by adsorption. The adsorbents used in the studies were synthesized from silica extracted from rice husk and they were MOR, MCM-41 (A) and MCM-41 (C). The rice husk silica was also used as the adsorbent.

Of all the adsorbents, MCM-41 (A) and MCM-41 (C) were found to be the best adsorbents for oleic acid. The equilibrium adsorption capacity at 25 °C of MCM-41 (A) was 277.8 mg/g and that of MCM-41 (C) was 270.3 mg/g. These were about 4 times higher than those obtained with MOR and silica. Surface area, active sites and appropriate pore size of the adsorbents are the factors that influence for the high adsorption capacity.

The adsorption of oleic acid onto MCM-41 (A) and MCM-41 (C) followed the Langmuir isotherm model. The adsorption processes were spontaneous and exothermic. After the equilibrium adsorption, the systems were in a higher state of randomness.

MCM-41 (A) could be used in the adsorption of oleic acid in soybean oil, although the adsorption capacity was lower due to the adsorption of triacylglycerol onto the adsorbent. To remove a higher amount of the acid from the oil, a larger amount of the adsorbent is recommended.

MCM-41 (A) is a good candidate to be used as the adsorbent for the removal of free fatty acid in the real oil samples, but several issues must be further investigated. The regeneration and reuse of the adsorbent are of interest for economic reasons. The reagent to be used should be investigated. The stability of the surfactant inside the pore of MCM-41 has to be evaluated. Species that might compete for the adsorption must be identified.
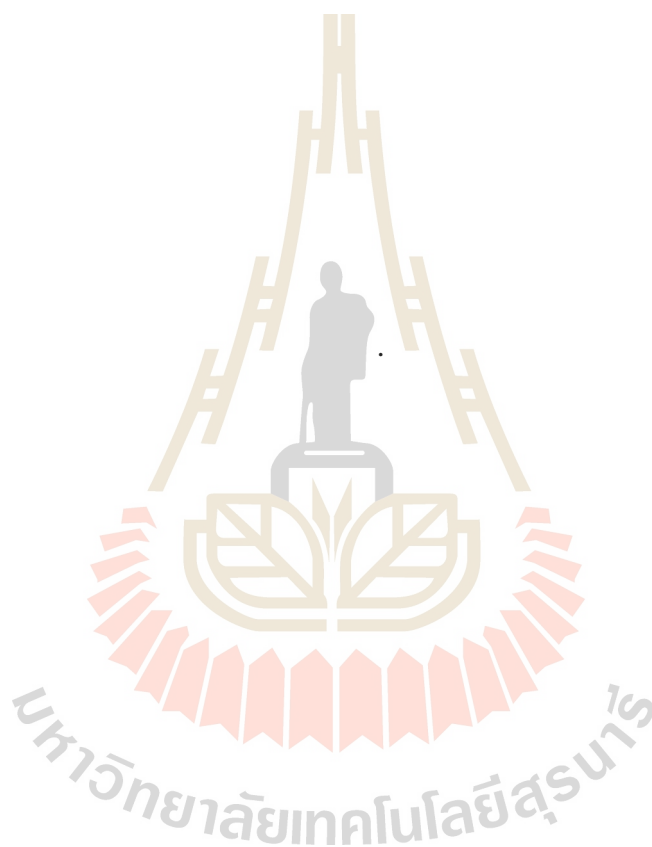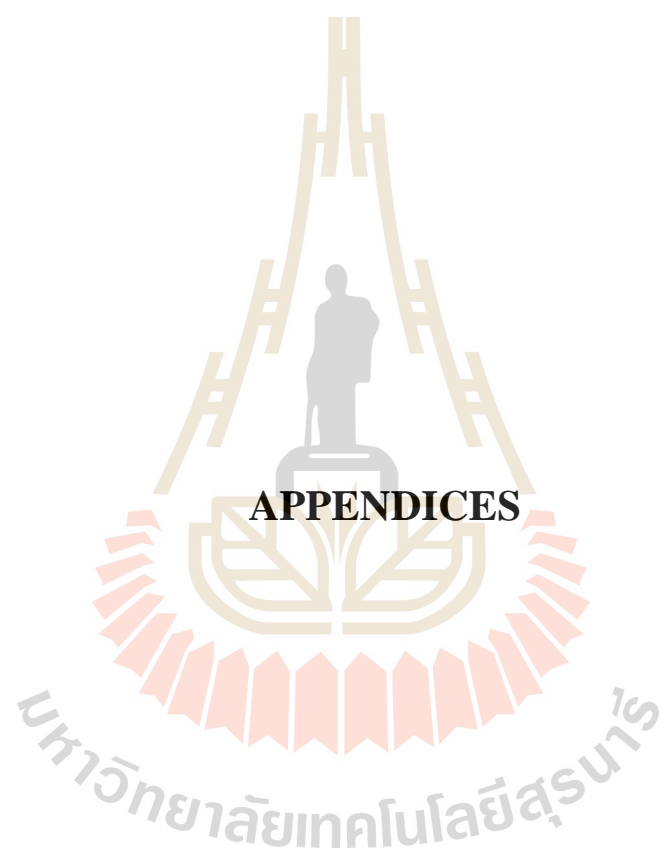
APPENDICES

APPENDIX A

DETERMINATION OF OLEIC ACID BY HPLC
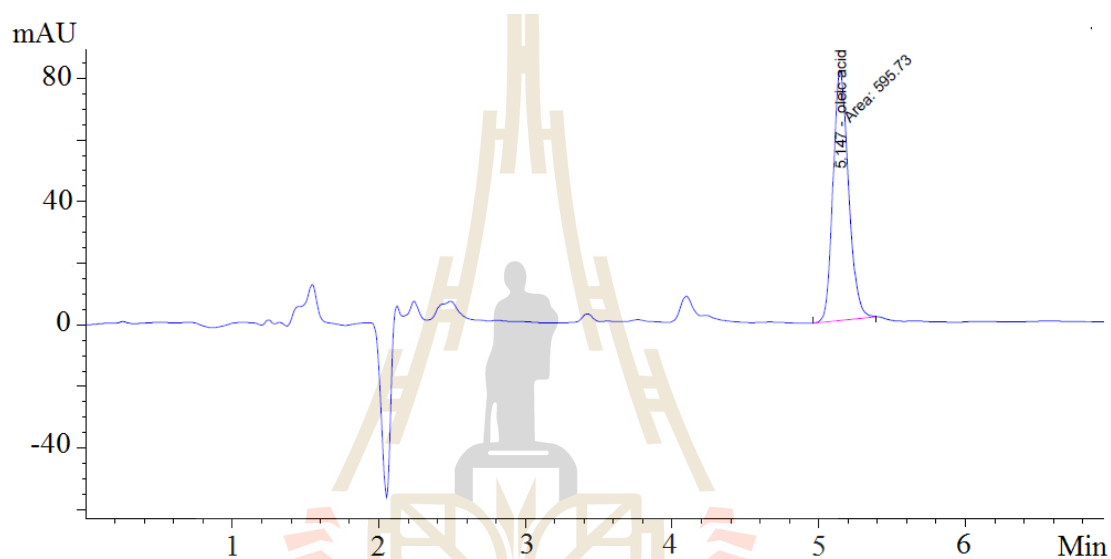
Figure A.1 A chromatogram of 22 ppm oleic acid. The mobile phase was acetonitrile mixed with 0.4% acetic acid in H_2O with the ratio 90:10. The mobile phase flow rate was 1 mL/min.
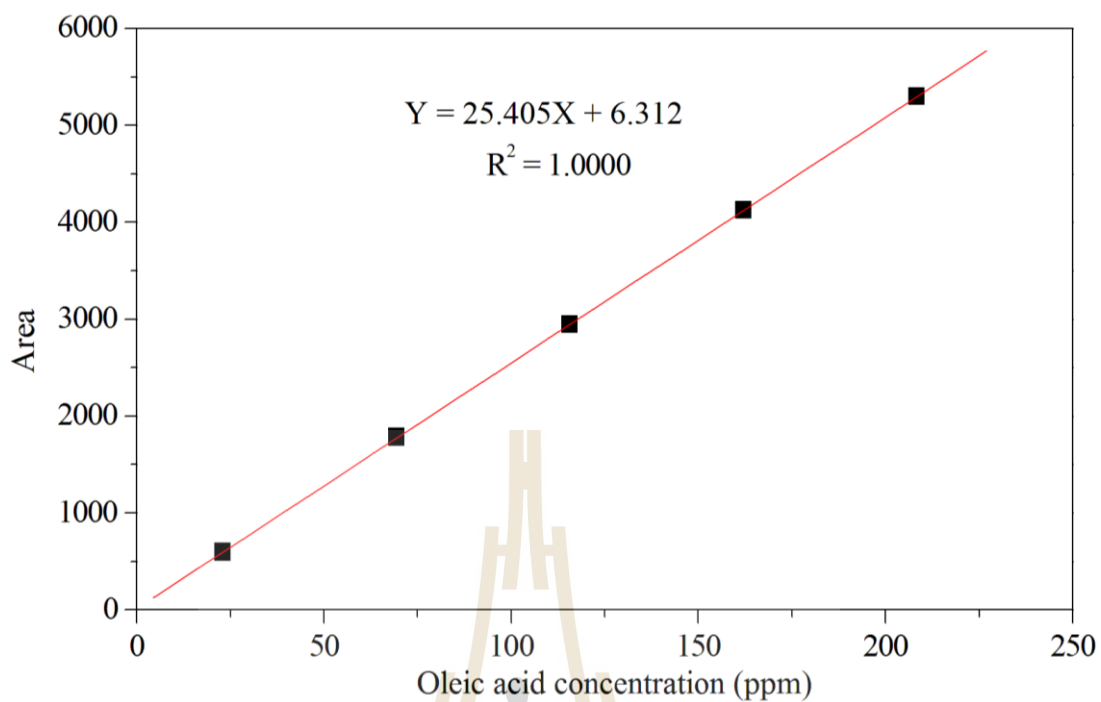
Figure A.2 A Calibration curve for the determination of oleic acid for the adsorption conducted at 25 °C.
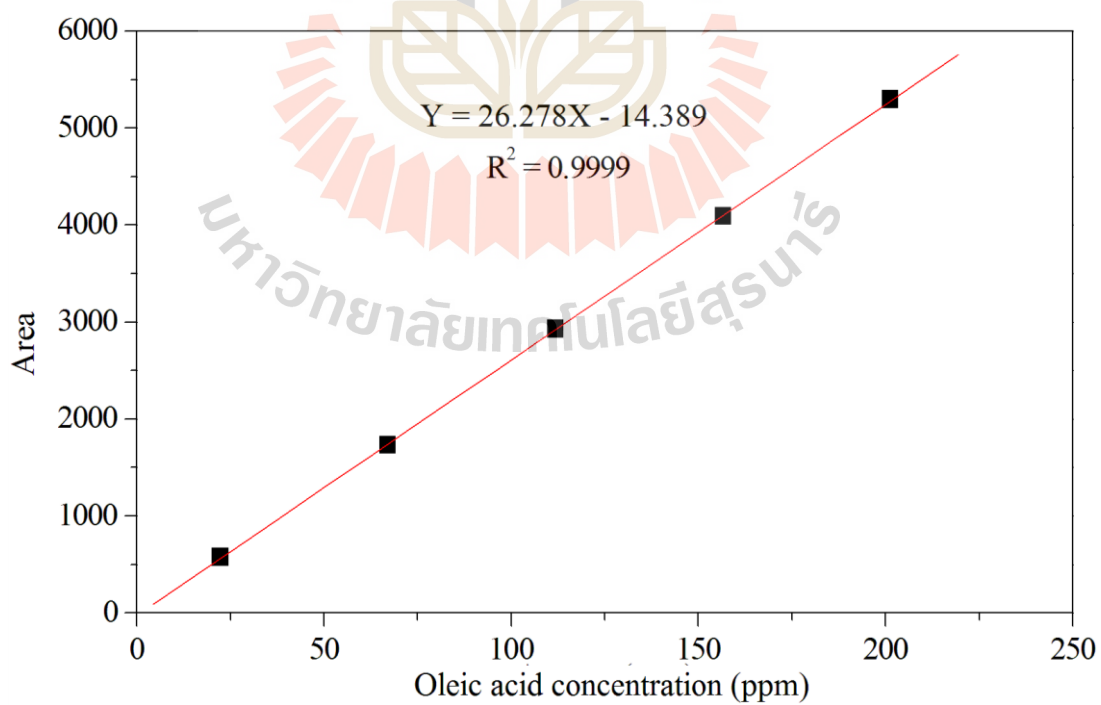
Figure A.3 A Calibration curve for the determination of oleic acid for the adsorption conducted at 30 °C.
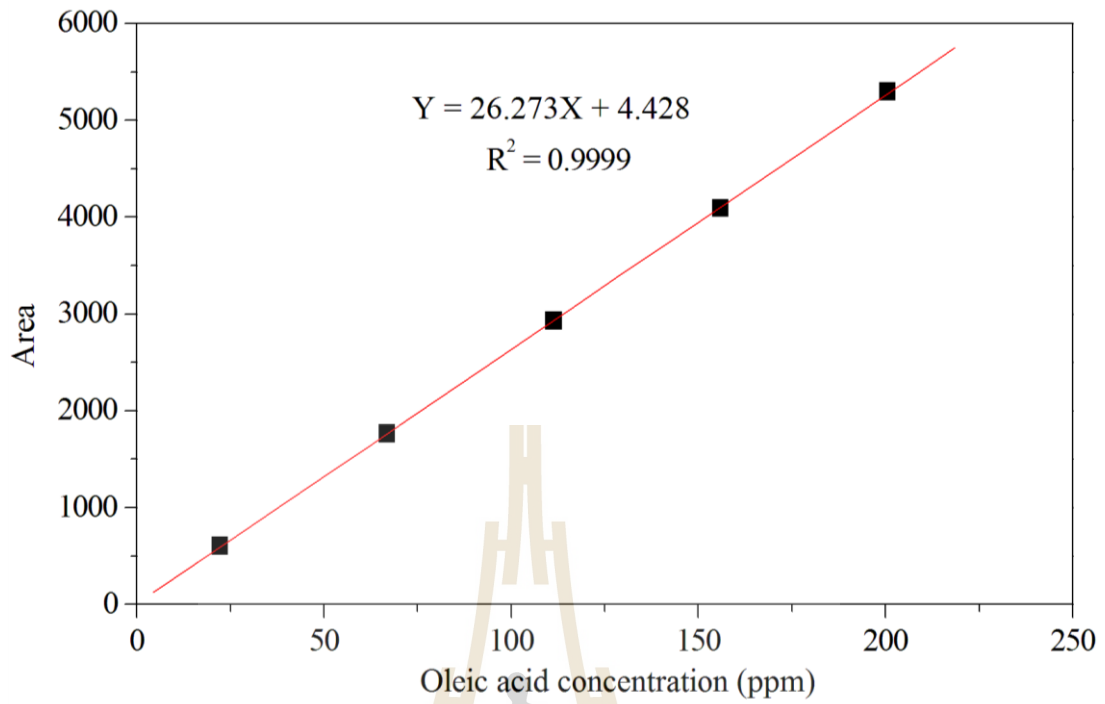
Figure A.4 A Calibration curve for the determination of oleic acid for the adsorption

conducted at 40 °C.

APPENDIX B

LANGMUIR AND FREUNDLICH ISOTHERM FITTING

FOR THE ADSORPTION OF OLEIC ACID ON MOR,

MCM-41 (A) AND MCM-41 (C)

$$Y = 0.011X + 182.9993$$
$$R^2 = 0.0224$$
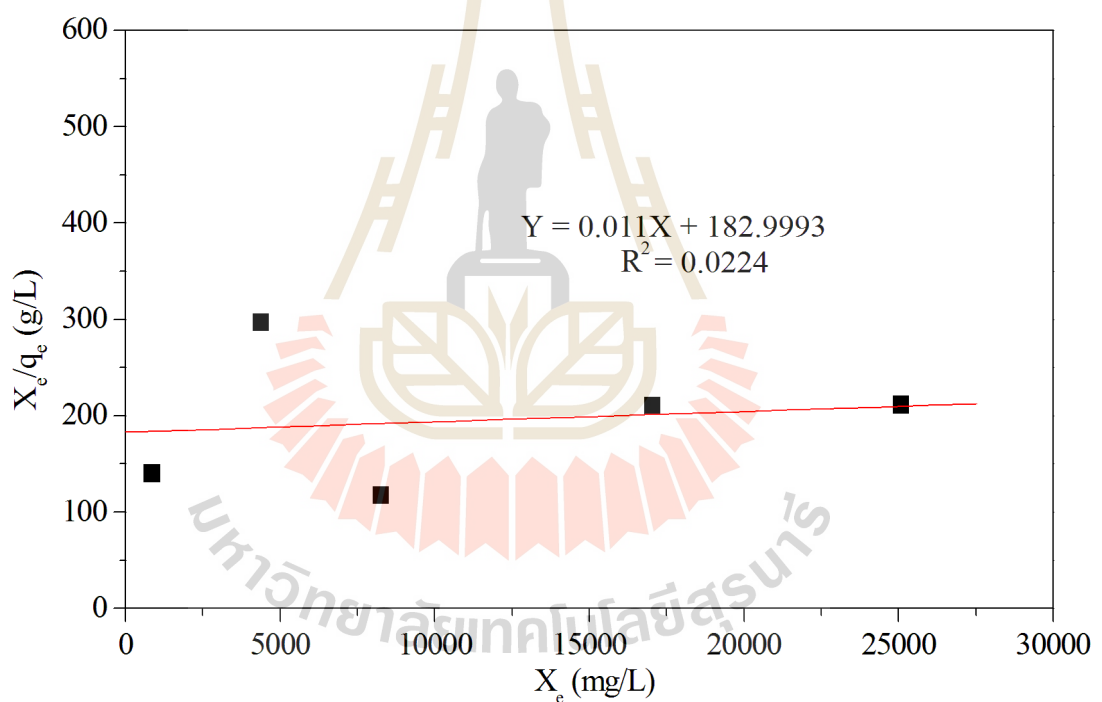
Figure B.1 The linear Langmuir isotherm fitting for oleic acid adsorption in isooctane onto MOR at 25 °C.
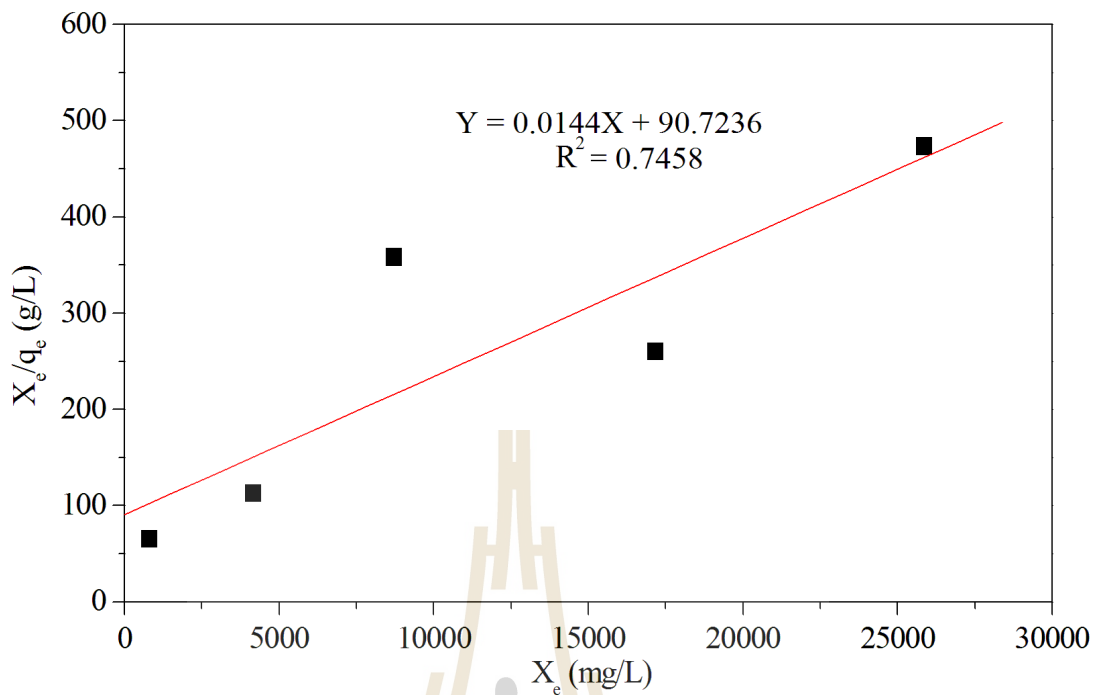
Figure B.2 The linear Langmuir isotherm fitting for oleic acid adsorption in isooctane onto MOR at 30 °C.
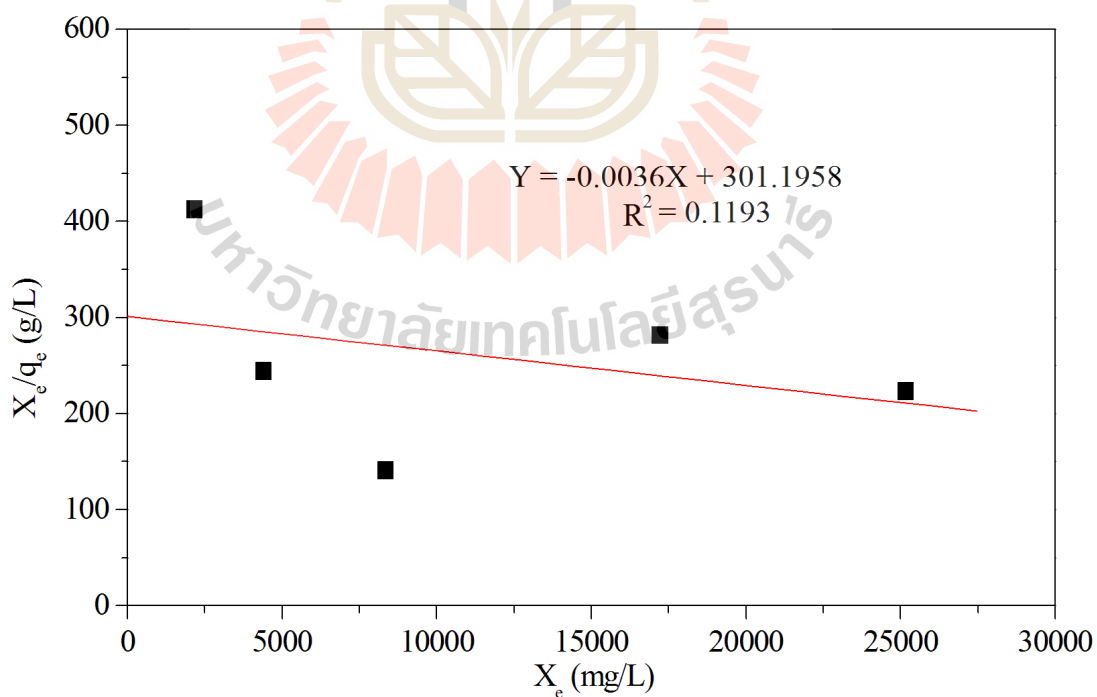
Figure B.3 The linear Langmuir isotherm fitting for oleic acid adsorption in isooctane onto MOR at 40 °C.
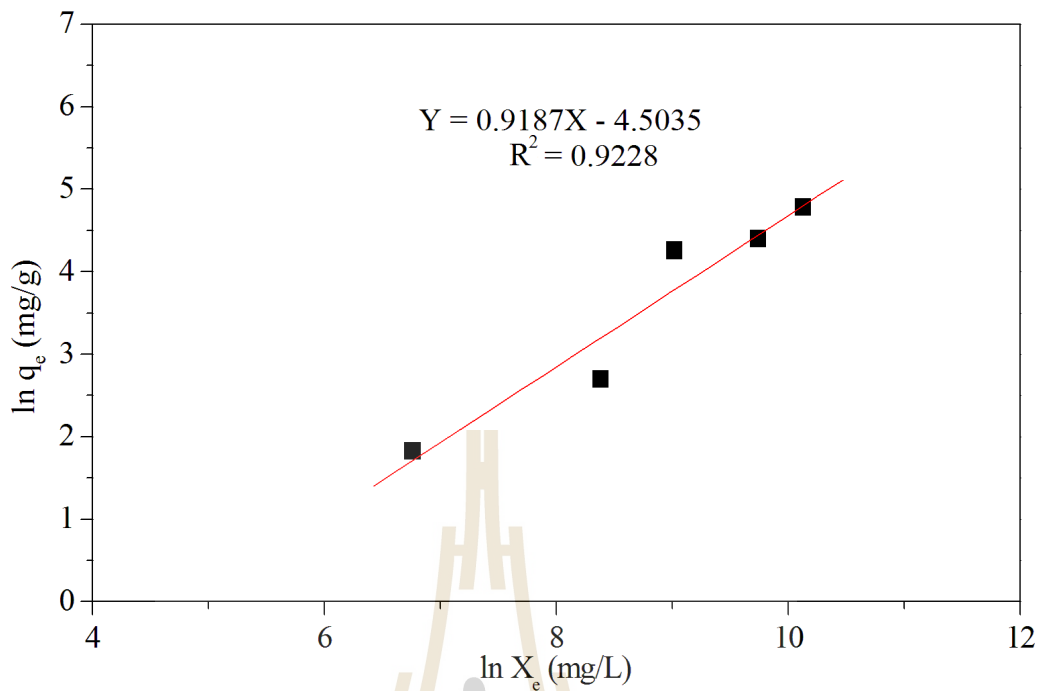
Figure B.4 The linear Freundlich isotherm fitting for oleic acid adsorption in isooctane
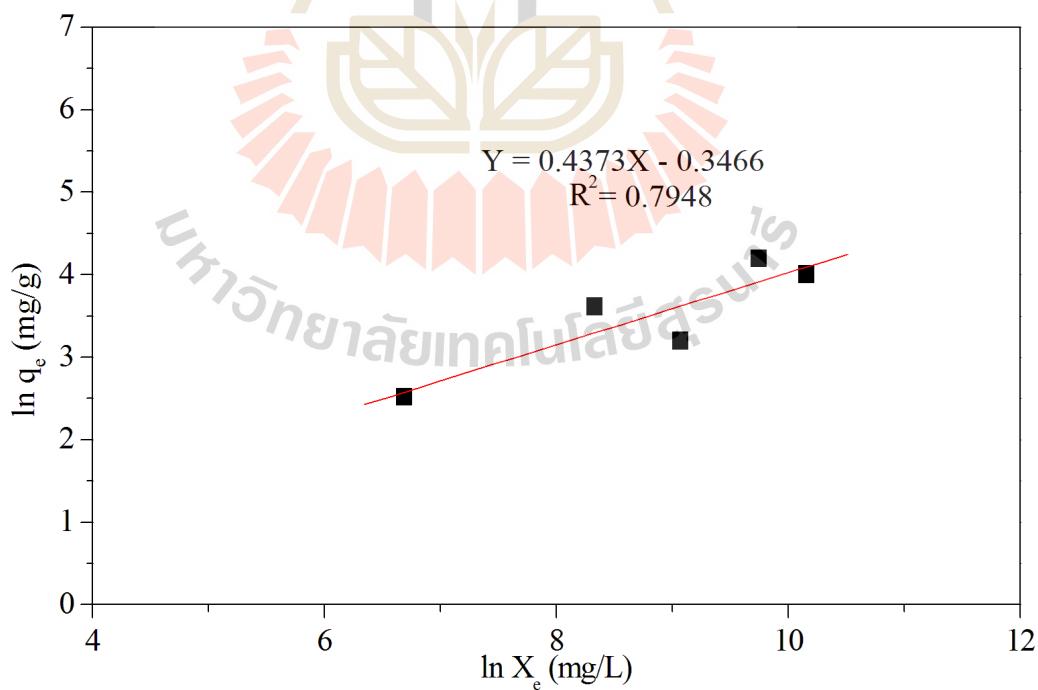
onto MOR at 25 °C.

Figure B.5 The linear Freundlich isotherm fitting for oleic acid adsorption in isooctane
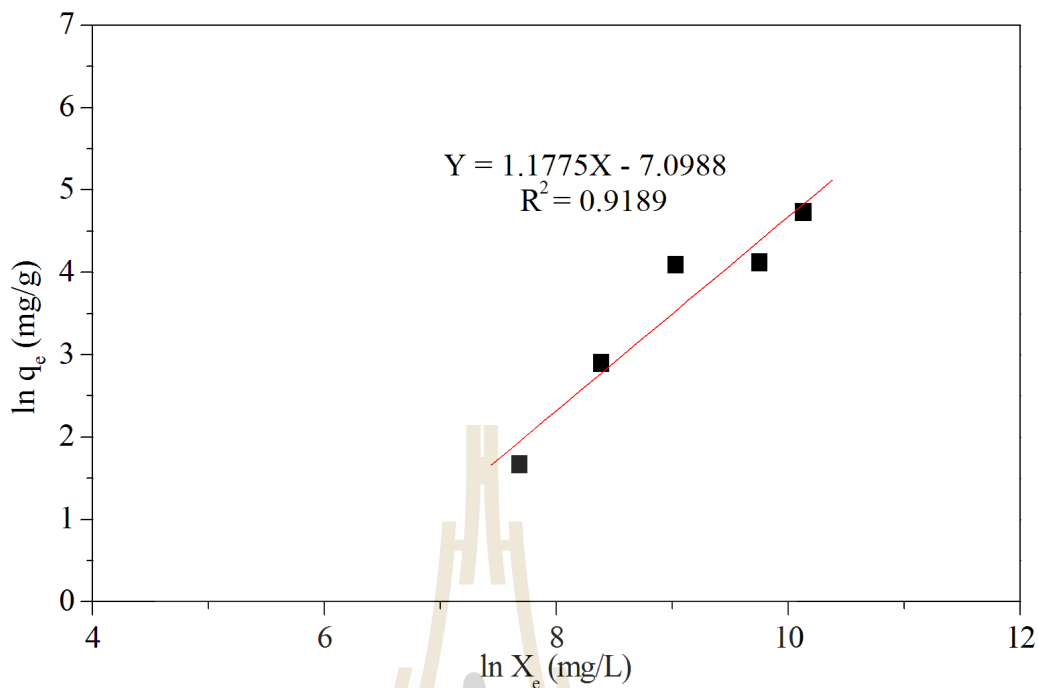
onto MOR at 30 °C.

Figure B.6 The linear Freundlich isotherm fitting for oleic acid adsorption in isooctane

onto MOR at 40 °C.
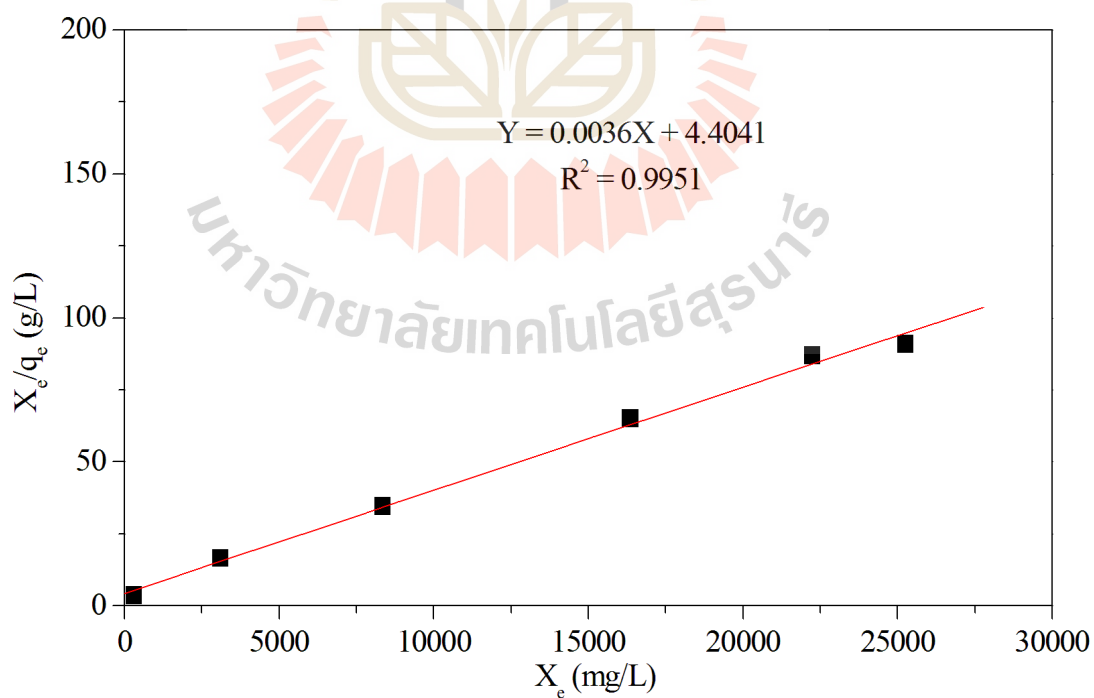
Figure B.7 The linear Langmuir isotherm fitting for oleic acid adsorption in isooctane
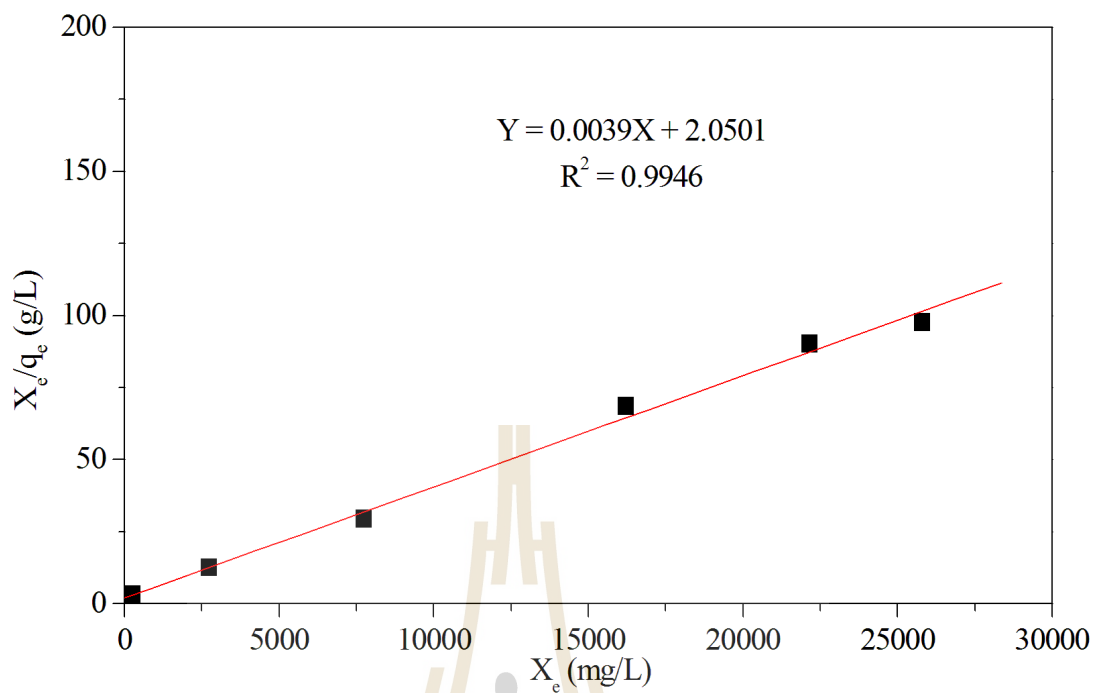
onto MCM-41 (A) at 25 °C.

Figure B.8 The linear Langmuir isotherm fitting for oleic acid adsorption in isooctane
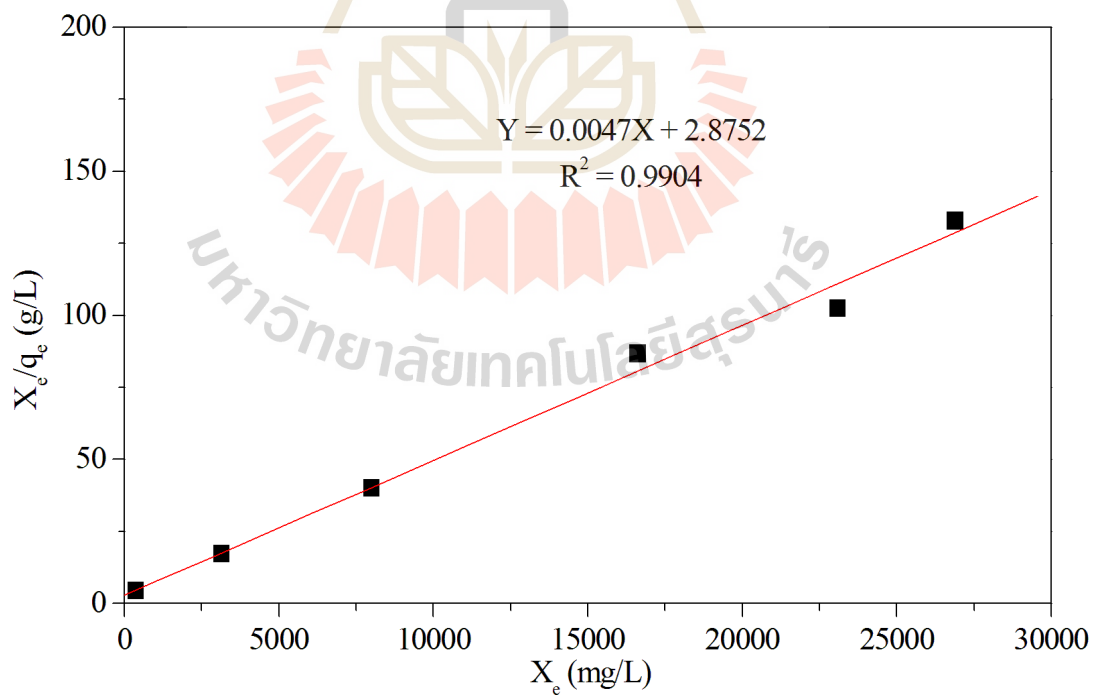
onto MCM-41 (A) at 30 °C.

Figure B.9 The linear Langmuir isotherm fitting for oleic acid adsorption in isooctane
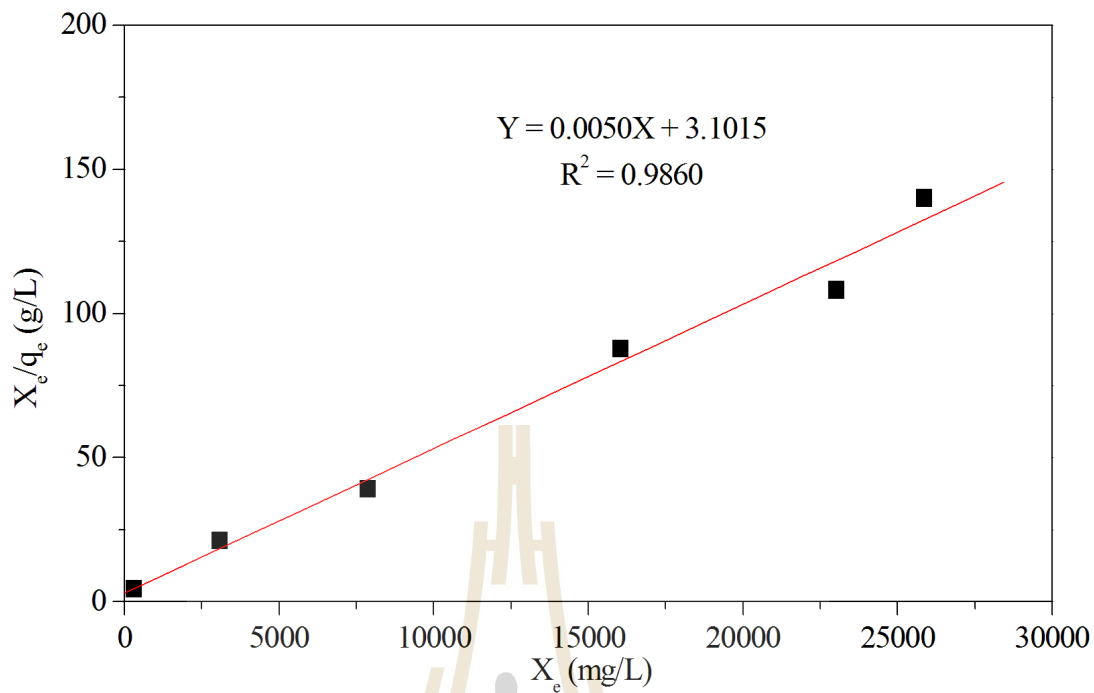
onto MCM-41 (A) at 40 °C.

Figure B.10 The linear Langmuir isotherm fitting for oleic acid adsorption in isooctane
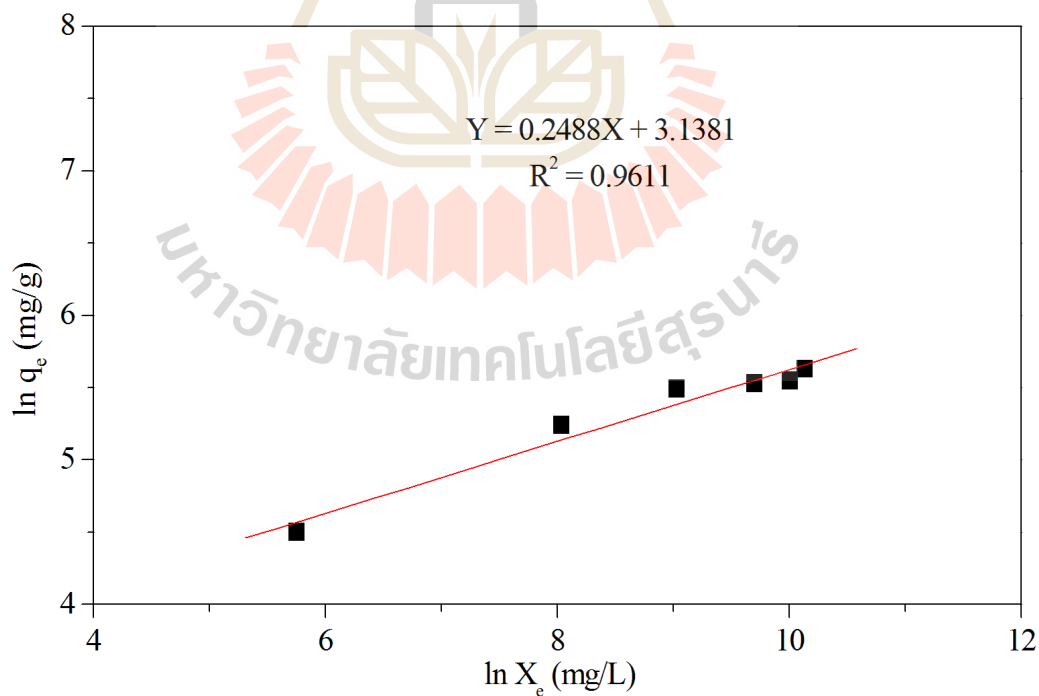
onto MCM-41 (A) at 50 °C.

Figure B.11 The linear Freundlich isotherm fitting for oleic acid adsorption in isooctane
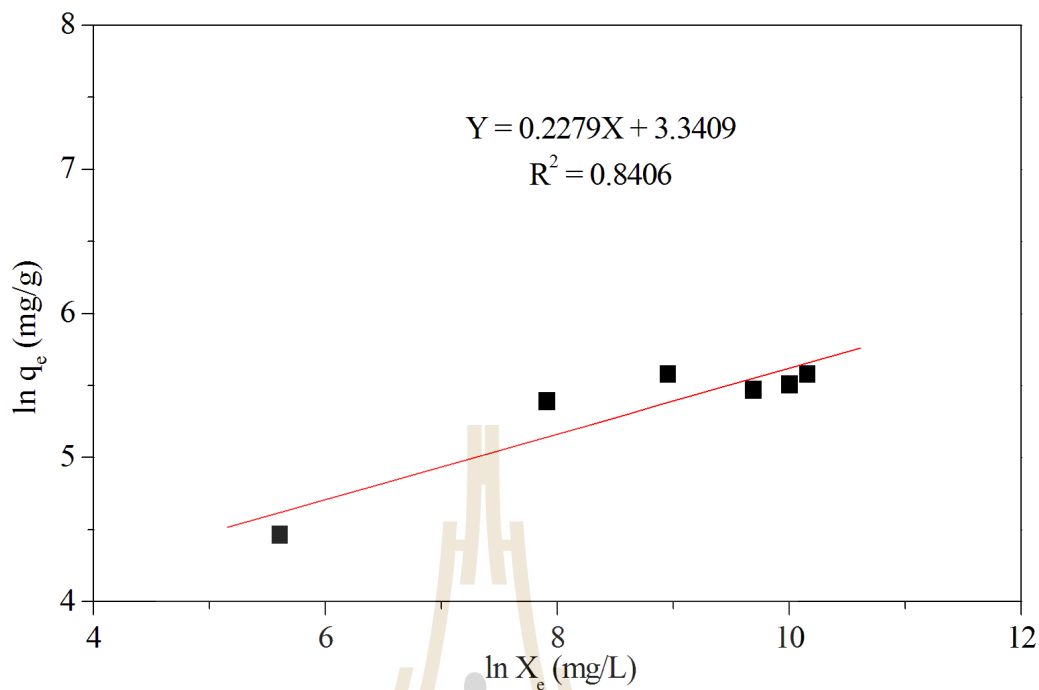
onto MCM-41 (A) at 25 °C.

Figure B.12 The linear Freundlich isotherm fitting for oleic acid adsorption in isooctane onto MCM-41 (A) at 30 °C.
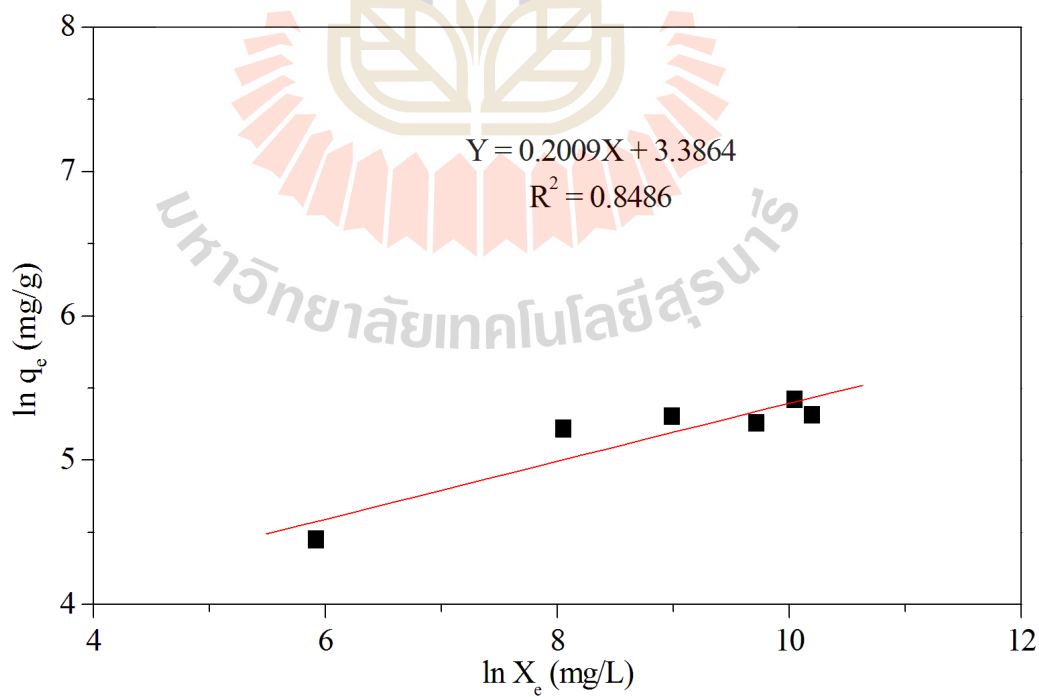
Figure B.13 The linear Freundlich isotherm fitting for oleic acid adsorption in isooctane onto MCM-41 (A) at 40 °C.
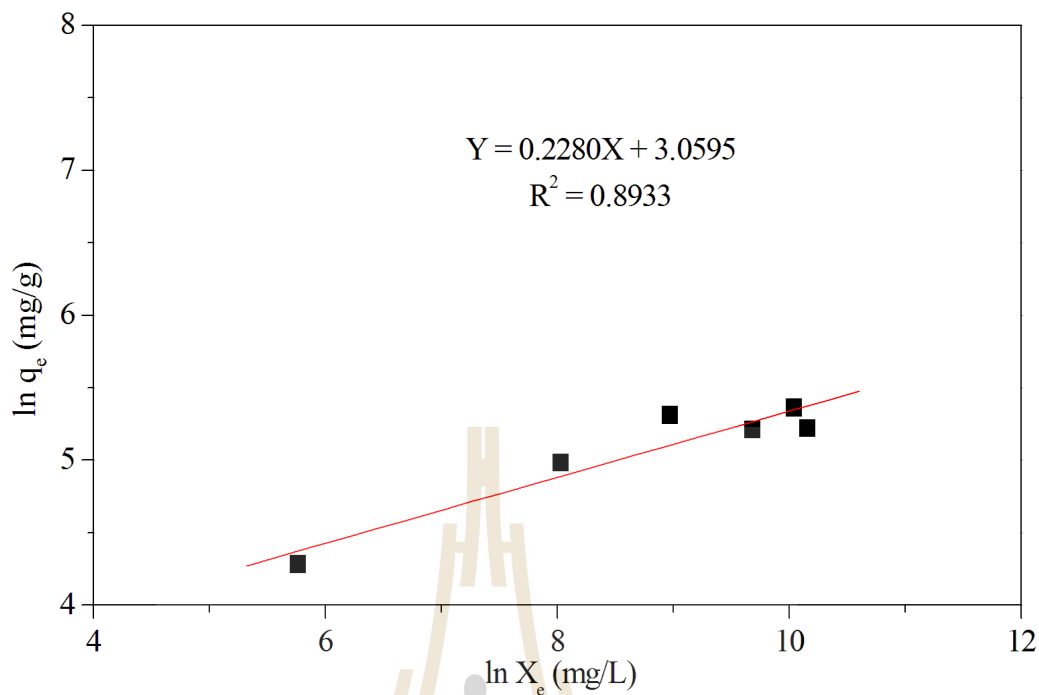
Figure B.14 The linear Freundlich isotherm fitting for oleic acid adsorption in isooctane

onto MCM-41 (A) at 50 °C.
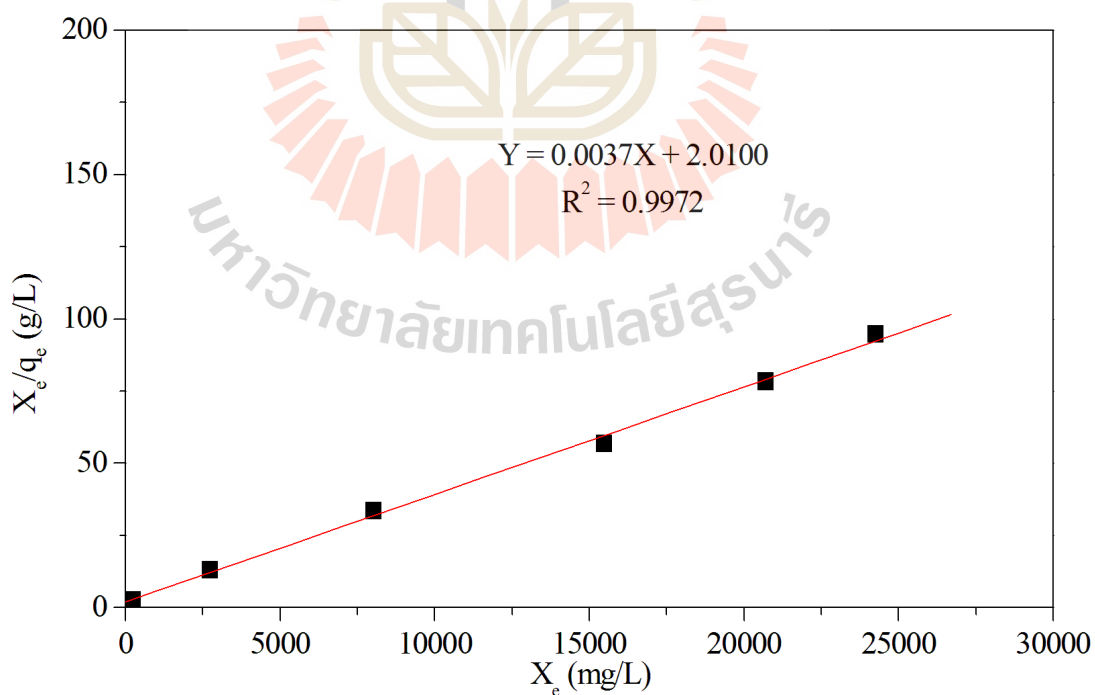
Figure B.15 The linear Langmuir isotherm fitting for oleic acid adsorption in isooctane
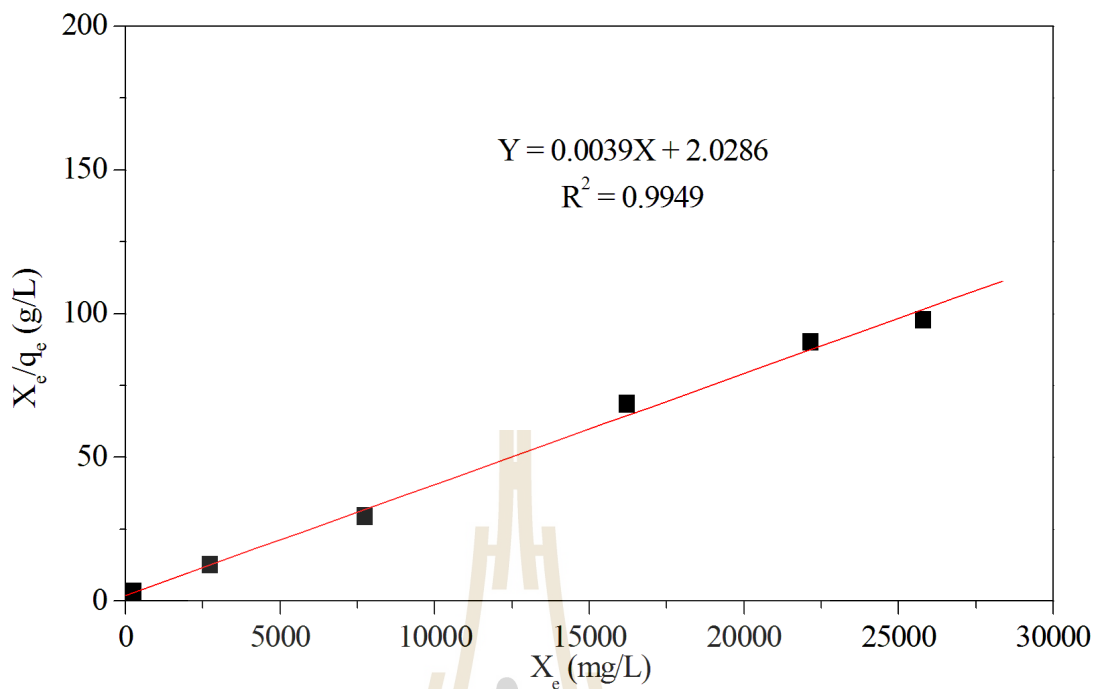
onto MCM-41 (C) at 25 °C.

Figure B.16 The linear Langmuir isotherm fitting for oleic acid adsorption in isooctane
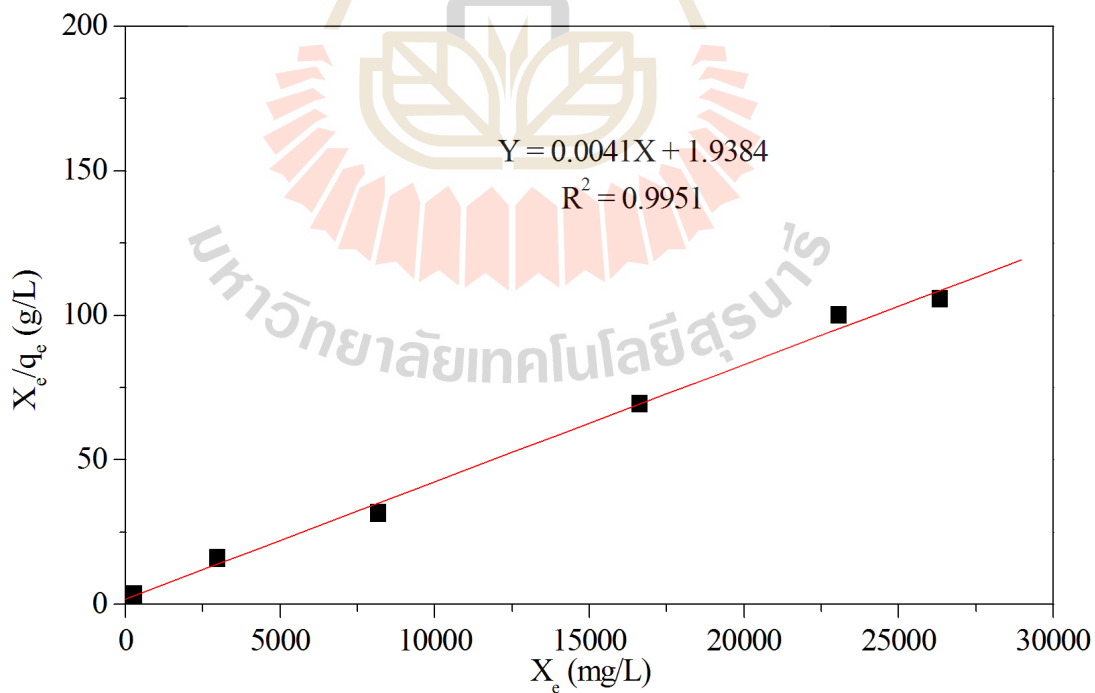
onto MCM-41 (C) at 30 °C.

Figure B.17 The linear Langmuir isotherm fitting for oleic acid adsorption in isooctane
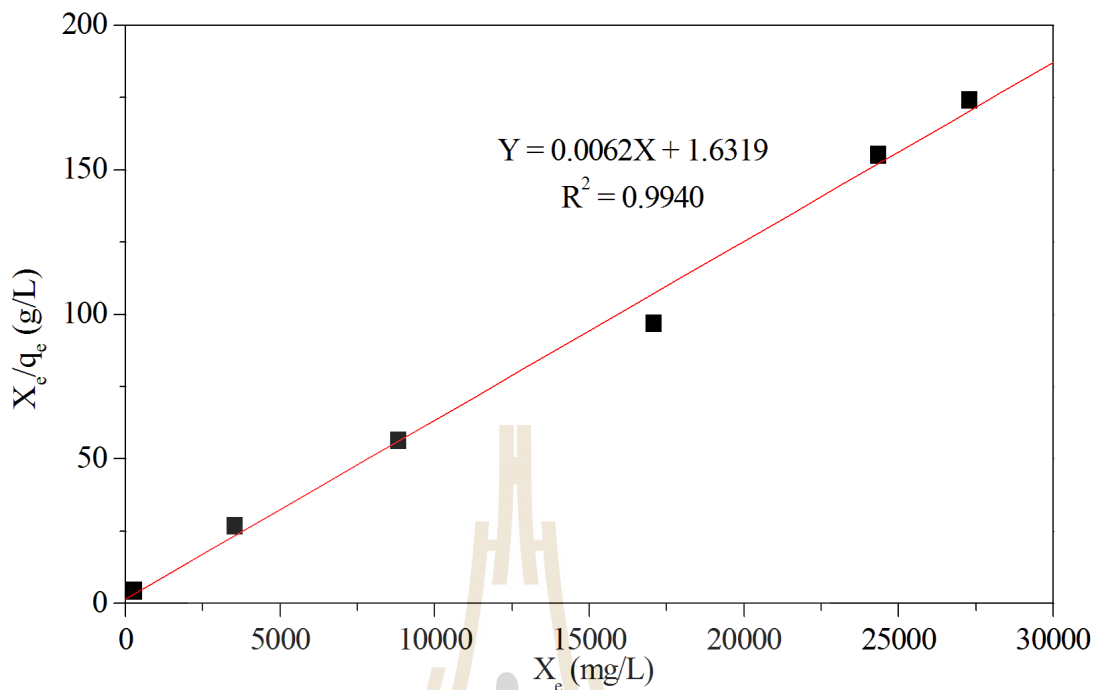
onto MCM-41 (C) at 40 °C.

Figure B.18 The linear Langmuir isotherm fitting for oleic acid adsorption in isooctane
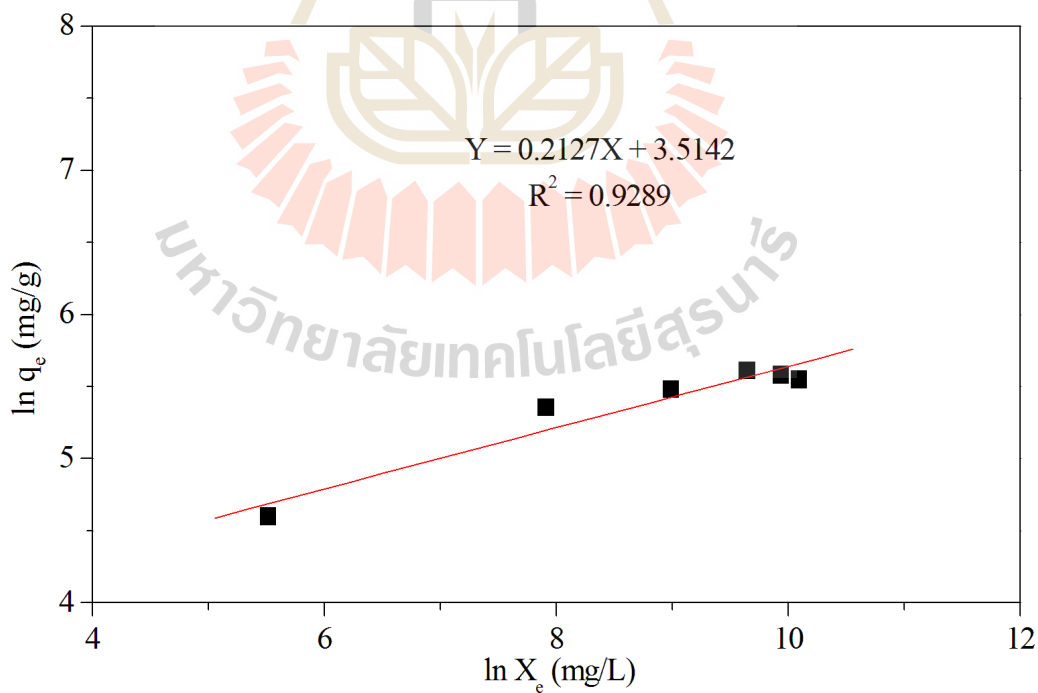
onto MCM-41 (C) at 50 °C.

Figure B.19 The linear Freundlich isotherm fitting for oleic acid adsorption in isooctane
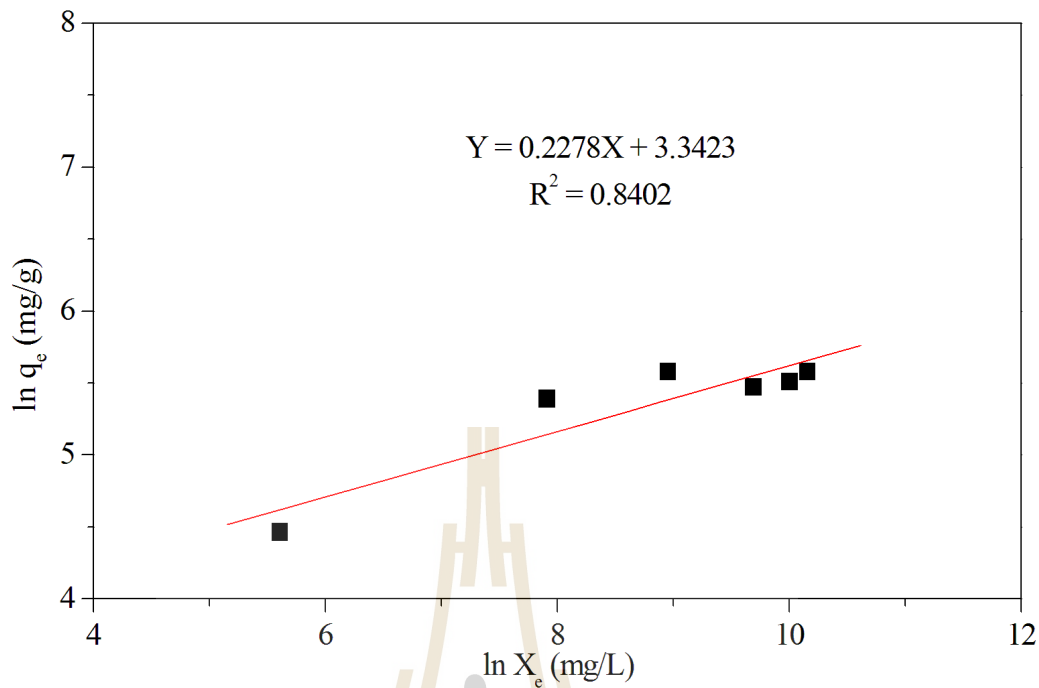
onto MCM-41 (C) at 25 °C.

Figure B.20 The linear Freundlich isotherm fitting for oleic acid adsorption in isooctane onto MCM-41 (C) at 30 °C.
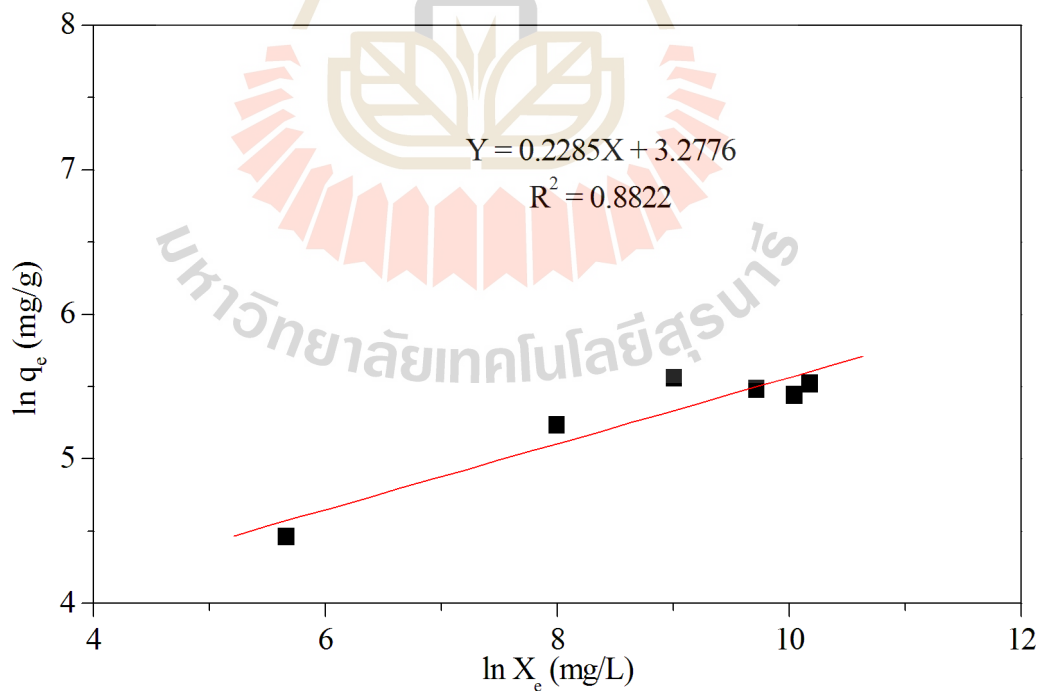
Figure B.21 The linear Freundlich isotherm fitting for oleic acid adsorption in isooctane onto MCM-41 (C) at 40 °C.
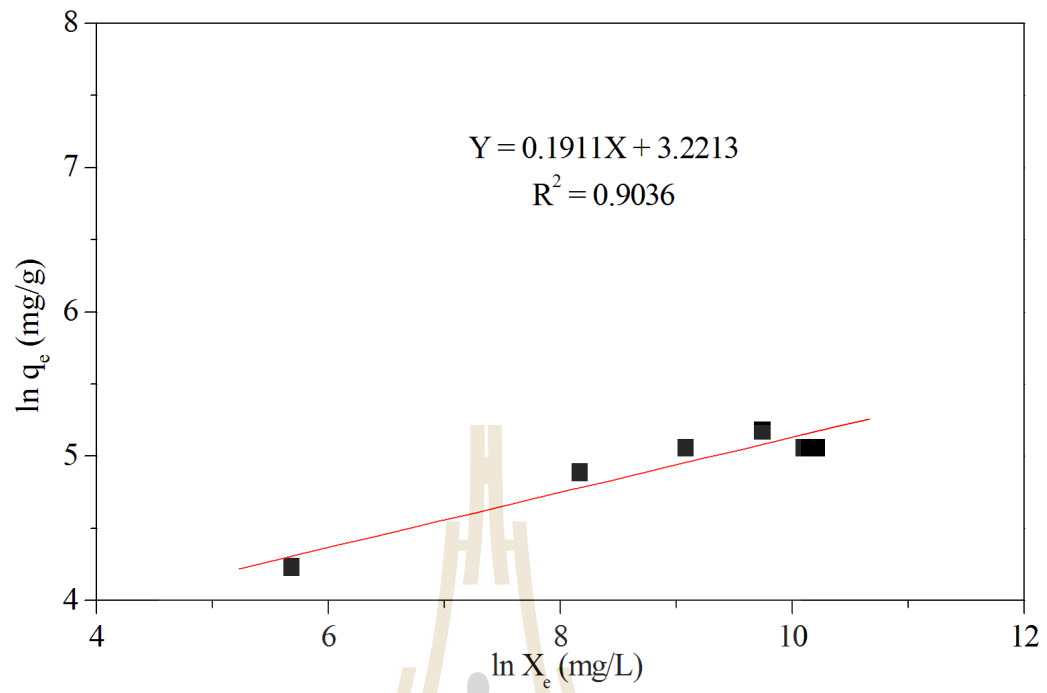
Figure B.22 The linear Freundlich isotherm fitting for oleic acid adsorption in isooctane

onto MCM-41 (C) at 50 °C.

APPENDIX C

DATA FROM N$_2$ ADSORPTION-DESORPTION

Table C-1 N$_2$ adsorption-desorption of silica.

Relative pressure (P/P$_0$)	Volume adsorbed (cm^3/g STP)	Relative pressure (P/P$_0$)	Volume adsorbed (cm^3/g STP)
0.000000013	0	0.653478514	129.2823
0.001708288	19.8701	0.7081059	147.6219
0.002946152	22.2167	0.74642756	159.1726
0.004988675	24.6016	0.799906231	173.3946
0.0071994	26.3404	0.850004544	184.6584
0.008673506	27.2626	0.89783705	194.7831
0.009981009	27.9743	0.944985799	207.4813
0.014373415	29.8997	0.989400265	237.3818
0.020214144	31.8126	0.949604504	214.7426
0.024824596	33.021	0.905604312	202.222
0.030068176	34.1979	0.850145788	192.4821
0.035177587	35.2197	0.78794791	182.8672
0.040348946	36.128	0.753312117	176.9085
0.045220927	36.8885	0.702289211	165.8819
0.050325298	37.6438	0.652689649	151.1662
0.054617906	38.2371	0.600091342	131.518
0.060300322	38.9749	0.552608324	107.6713
0.065402732	39.5978	0.494527493	80.7104
0.070374796	40.1712	0.449902852	72.071
0.074760326	40.6591	0.39352288	65.6271
0.079720475	41.1857	0.355784751	62.2932
0.085478264	41.7795	0.301706172	57.9019
0.090262974	42.2525	0.25075007	54.0504
0.09529962	42.7376	0.201701381	50.4551
0.100398097	43.2056	0.151125754	46.5563
0.143881694	46.9087	0.101162277	42.2716
0.199897765	51.2036	0.09148597	41.3276
0.250843512	54.9171	0.081608012	40.3127
0.301290036	58.6767	0.071501555	39.1916
0.349969103	62.5522	0.060984454	37.9197
0.399809201	66.9078	0.051076363	36.5788
0.450064214	71.8106	0.040913091	34.994
0.49865569	78.0007	0.030404803	32.9945
0.546787747	87.8003	0.020532475	30.5213
0.594963444	105.0886	0.009859249	26.2771

Table C-2 N_2 adsorption-desorption of MOR.

Relative pressure (P/P$_0$)	Volume adsorbed (cm^3/g STP)	Relative pressure (P/P$_0$)	Volume adsorbed (cm^3/g STP)
0.000028854	10.1692	0.570284310	102.7802
0.000030532	20.3499	0.620440655	102.6582
0.000027291	30.7982	0.670335756	102.5267
0.000027751	41.5091	0.720256438	102.4181
0.000027907	52.6045	0.770300623	102.3222
0.000027338	63.9667	0.820203762	102.2457
0.000384539	75.3725	0.870105115	102.2401
0.001101226	90.5541	0.919760840	102.3987
0.004083822	95.1174	0.950259226	102.8254
0.005109494	96.4286	0.987183904	105.2594
0.007442980	97.8372	0.935966118	103.0781
0.008987490	98.6129	0.881923810	102.8758
0.009660438	99.2485	0.831426834	102.9212
0.016849499	99.7342	0.987183904	105.2594
0.020863996	100.8704	0.781022814	103.0869
0.027439784	101.5198	0.730902538	103.3204
0.034195122	101.7884	0.680838310	103.5526
0.039688724	102.1958	0.630843106	103.7907
0.040559266	102.2939	0.580748871	104.0266
0.046472639	102.3739	0.530709657	104.2579
0.057276760	102.6161	0.480681268	104.4520
0.060788715	102.6924	0.430580545	104.6184
0.065171477	102.8787	0.380479232	104.8176
0.070573580	102.9955	0.330422384	104.9997
0.075865477	103.0403	0.280399176	105.1505
0.080573265	103.1393	0.230366358	105.2976
0.085445865	103.1990	0.180269678	105.4273
0.090518111	103.2616	0.130293924	105.5112
0.095512976	103.3128	0.085578217	105.4349
0.100483588	103.3638	0.080383042	105.3972
0.150518894	103.3944	0.070458730	105.3356
0.200392996	103.4898	0.060497706	105.2484
0.250809183	103.4126	0.050386765	105.1456
0.300710424	103.3574	0.040553314	104.9796
0.370538921	103.1982	0.030305451	104.7198
0.420424494	103.1181	0.020388371	104.3401
0.470483325	103.0118	0.010025056	103.4953
0.520377873	102.8737		

92

Table C-3 N_2 adsorption-desorption of MCM-41 (A).

Relative pressure (P/P_0)	Volume adsorbed $(cm^3/g\ STP)$	Relative pressure (P/P_0)	Volume adsorbed $(cm^3/g\ STP)$
0.000026988	10.1490	0.499226047	561.7360
0.000032115	20.3009	0.549588230	565.1815
0.000043850	30.4493	0.599643641	568.3279
0.000065155	40.5927	0.649691643	571.2903
0.000099287	50.7318	0.699512208	574.2031
0.000151479	60.8655	0.749617923	577.2062
0.000229727	70.9920	0.799493793	580.4002
0.000344986	81.1086	0.848901326	584.1197
0.000512620	91.2122	0.897997115	589.0818
0.000753300	101.3018	0.943973247	597.5264
0.001097121	111.3590	0.987474724	628.6470
0.002924612	138.9697	0.950442443	604.0737
0.004790120	153.5355	0.895231375	590.3678
0.006678593	163.9721	0.846498071	585.0258
0.008701195	172.3924	0.792922068	580.8517
0.009673880	175.8875	0.752966012	578.2075
0.014383794	189.0933	0.700773997	575.0389
0.019864169	200.6080	0.650314564	572.0697
0.024143424	208.0075	0.600319986	569.0723
0.029645123	216.2180	0.549992859	565.9352
0.034939012	223.1310	0.500132740	562.5979
0.038718638	227.6775	0.451562167	558.4556
0.043540278	233.0356	0.399106070	553.3308
0.048841708	238.4873	0.350837596	547.5616
0.054326841	243.7575	0.302167419	505.0304
0.057132867	246.3138	0.255387243	397.0065
0.064365577	252.5615	0.196969770	337.0826
0.069920016	257.0916	0.153497918	310.8415
0.074885407	260.9726	0.104516546	281.3176
0.079808252	264.6680	0.091040188	272.2945
0.084756945	268.2784	0.080340935	264.6910
0.089705885	271.7614	0.070863834	257.4746
0.094649083	275.1551	0.062724904	250.4515
0.099618207	278.4248	0.050252594	238.8700
0.146212065	306.8467	0.041239252	229.2842
0.195503390	336.0095	0.030710200	216.0502
0.243519302	376.4141	0.020941062	200.4016
0.295525987	480.1903	0.010391575	174.6214
0.378088508	550.9572	0.000026988	0.0000
0.409780762	554.3421	0.000032115	0.0000
0.457311246	558.5308	0.000043850	0.0000

Table C-4 N_2 adsorption-desorption of MCM-41 (C).

Relative pressure (P/P_0)	Volume adsorbed $(cm^3/g \text{ STP})$	Relative pressure (P/P_0)	Volume adsorbed $(cm^3/g \text{ STP})$
0.000784740	20.1063	0.700206588	171.0088
0.002963059	29.7632	0.750267766	172.4202
0.003015970	29.9468	0.800142286	174.0133
0.005022095	34.4867	0.849982682	175.9965
0.006677797	37.3931	0.899122912	178.8825
0.008721066	40.3433	0.946741085	184.3016
0.009734463	41.6556	0.986347751	204.1644
0.015896044	47.5375	0.949317714	187.1539
0.020495132	50.9299	0.899688601	180.0314
0.024629974	53.5383	0.840348422	176.5435
0.029986982	56.5316	0.786401989	174.5137
0.035202499	59.0660	0.752819946	173.4696
0.039968356	61.1935	0.701051256	172.0528
0.045234130	63.3113	0.650859435	170.7928
0.050110201	65.1282	0.600859183	169.5670
0.053263868	66.2948	0.550720505	168.3316
0.060297831	68.5818	0.500772077	167.0565
0.065104095	70.0835	0.451285910	165.4787
0.070031715	71.5491	0.400154107	163.7060
0.074973010	72.9555	0.350831219	161.7476
0.079941542	74.3199	0.301822200	158.9985
0.084779640	75.6177	0.245042180	137.5143
0.089785273	76.9132	0.203267334	114.9707
0.094705195	78.1533	0.134969353	94.7741
0.099625964	79.3632	0.104758390	87.5546
0.144028051	89.0829	0.093356957	84.6146
0.193768726	101.3300	0.080000646	81.0071
0.251289248	131.3276	0.070316969	78.1709
0.300179792	156.7758	0.060156720	74.9713
0.404667181	162.6364	0.050384460	71.5494
0.464841225	164.6467	0.040234045	67.4893
0.516131369	166.1539	0.030398203	62.8548
0.549916054	167.0951	0.020720154	57.1300
0.600457373	168.4086	0.010451647	48.4112
0.650165890	169.6889		

CURRICULUM VITAE

Name: Miss Benjaluck Narachai

Date of Birth: September 17th, 1981 in Amnatcharoen, Thailand

E-mail: tawanok@hotmail.com

Telephone: 085-3314497

Education:

2000-2003 B.Sc. (Chemistry), Ubon Ratchathani University

Work experience

June 3, 2004-Mar 11, 2005;

Quality Assurance (Q.A), Community Pharmacy Public Co., Ltd

Mar 16, 2005-Dec 30, 2005;

Research & Development (R&D)

Pan Rajdhevee Group Public Company Limited

Jan 4, 2006-Feb 19, 2009;

Senior Production Engineer, NEC/TOKIN Electronics (Thailand) Co.,

Ltd